RM L52J10
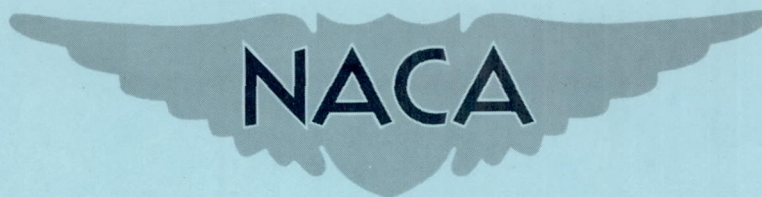
NACA RM L52J10

NACA

RESEARCH MEMORANDUM

EFFECTS OF SWEEPBACK AND TAPER ON THE FORCE AND

CAVITATION CHARACTERISTICS OF ASPECT-RATIO-4 HYDROFOILS

By Douglas A. King and Norman S. Land

Langley Aeronautical Laboratory
Langley Field, Va.

NATIONAL ADVISORY COMMITTEE
FOR AERONAUTICS

WASHINGTON

December 2, 1952
Declassified October 29, 1954

NATIONAL ADVISORY COMMITTEE FOR AERONAUTICS

RESEARCH MEMORANDUM

EFFECTS OF SWEEPBACK AND TAPER ON THE FORCE AND

CAVITATION CHARACTERISTICS OF ASPECT-RATIO-4 HYDROFOILS

By Douglas A. King and Norman S. Land

SUMMARY

An investigation was made in Langley tank no. 2 to determine the effects of sweepback and taper ratio on the cavitation and hydrodynamic force characteristics of hydrofoils. Four hydrofoils were used, three having a taper ratio of 0.6 with 0°, 45°, and 60° sweepback of the quarter-chord line, and the fourth having 45° sweep and a taper ratio of 0.3. All hydrofoils had an aspect ratio of 4 and NACA 65A006 airfoil sections in the streamwise direction.

In order to eliminate the effects of the free-water surface and the interference of supporting struts, the tests were made with semispan models mounted vertically in the water on a reflection plate similar to wind-tunnel-wall mountings of semispan models.

Increasing the sweepback of the hydrofoils from 0 to 45° resulted in an increase in cavitation speed, but a further increase to 60° of sweep was of little or no additional benefit. Sweepback decreased lift-drag ratios both in the cavitating and noncavitating conditions. A change in taper ratio from 0.6 to 0.3 on a hydrofoil with 45° of sweepback resulted in only negligible effects on the cavitating speed and the force characteristics. The cavitation speed of the unswept hydrofoil at moderate and high lift coefficients was higher than that computed from theoretical pressure distributions, probably because of boundary-layer separation. The variation of cavitation speed with lift coefficient of the swept hydrofoils was similar to that of the unswept hydrofoil.

The hydrodynamic characteristics of the hydrofoils at subcavitation speeds were in reasonable agreement with the aerodynamic characteristics of similar wings, and the effects of sweep and taper on the subcavitation hydrodynamic characteristics were approximately the same as for wings.

INTRODUCTION

Large angles of sweep have been used to reduce the maximum pressure coefficient of wings and thereby increase the critical Mach number and alleviate the force breaks of such wings. Since the inception of cavitation on hydrofoils in water is similarly related to the minimum pressure peaks, it would appear that sweep could be used to advantage to increase the speed at which cavitation begins and possibly to improve performance under cavitating conditions.

A preliminary investigation has accordingly been made in Langley tank no. 2 of the effects of sweepback angle on the forces and flow characteristics of simple hydrofoils at speeds up to 90 feet per second and Reynolds numbers up to 1.5×10^6. The hydrofoils had NACA 65A006 sections in the streamwise direction, an aspect ratio of 4, and were considered favorable for operation at supercavitation speeds. The plan forms used were selected from the transonic-wing plan-form series extensively investigated aerodynamically by the National Advisory Committee for Aeronautics (ref. 1). They included sweepback angles of $0°$, $45°$, and $60°$ with a taper ratio of 0.6, and a sweepback angle of $45°$ with a taper ratio of 0.3.

The hydrofoils were tested as semispan models mounted vertically below a horizontal reflection plate submerged in the tank. This setup minimized possible surface effects and supporting-strut interferences and enabled a direct correlation of the data with those obtained similarly with wind-tunnel-wall balances.

SYMBOLS

A aspect ratio, $\dfrac{(2b)^2}{2S}$

b span of model, ft

C_D drag coefficient, $\dfrac{\text{Model drag}}{qS}$

C_L lift coefficient, $\dfrac{\text{Model lift}}{qS}$

$C_{m_{\bar{c}/4}}$ pitching-moment coefficient referred to $\bar{c}/4$, $\dfrac{\text{Model pitching moment}}{qS\bar{c}}$

H   free-stream total pressure, lb/sq ft

M   Mach number

p_{min} minimum value of local static pressure, lb/sq ft

p_o free-stream static pressure, lb/sq ft

p_v vapor pressure, lb/sq ft

q   dynamic pressure, $\frac{1}{2}\rho V^2$, lb/sq ft

R   Reynolds number, $\frac{V\bar{c}}{\nu}$

S   area of model, sq ft

S_{max} pressure coefficient corresponding to minimum value of local static pressure, $\frac{H - p_{min}}{q}$

V   free-stream speed, ft/sec

V_c cavitation speed, speed at which cavitation first appears on hydrofoil, ft/sec

$\bar{c}$ mean aerodynamic chord, ft

α   angle of attack, deg

ρ   mass density of water, 1.97 slug/cu ft for these tests

ν   kinematic viscosity of water, 1.21×10^{-5} sq ft/sec for these tests

MODELS

A semispan model of each hydrofoil was tested. Each had an NACA 65A006 airfoil section (see table I) parallel to the free-stream velocity, an area of $\frac{1}{16}$ square foot, and an aspect ratio of 4. In the same manner as in reference 1, the hydrofoils are designated by the

plan-form variables, sweep, aspect ratio, and taper ratio. Photographs
and dimensioned sketches of the models are shown in figures 1 and 2,
respectively.

In order to withstand the hydrodynamic lift loading, which was
expected to attain a value of about 2100 pounds per square foot (1 atmos-
phere), the hydrofoils were made of heat-treated chrome-vanadium steel
having a modulus of elasticity of approximately 30×10^6. After shaping
to the required size to a tolerance of ±0.003 inch on the section coordi-
nates, the surfaces were polished and electroplated. The 60-4-0.6 hydro-
foil was nickel-plated and the others were plated with chromium, all to
a thickness of about 0.001 inch for protection against corrosion.
Although the plating on all the hydrofoils except that on the 45-4-0.3
deteriorated during the tests, check tests showed negligible effects of
the change in surface on the characteristics of the hydrofoils.

APPARATUS

The tests were made in Langley tank no. 2 by using a special towing
gear. The towing gear, shown in figures 3 and 4, was based on the wall
mounting of semispan models in wind tunnels and consisted of a stainless-
steel reflection plate at the root chord of the hydrofoils supported below
the water by a hollow stainless-steel fairing and a framework attached
to the towing carriage. The fairing enclosed the balance staff and the
mounting flanges of the models. A circular portion of the reflection
plate rotated with change in angle of attack of the model but was not
connected to it. Photographs of two of the models on the towing gear
are shown in figure 5.

The models were mounted on a three-component, electrical-resistance,
strain-gage balance with the axis of the balance at the 25-percent sta-
tion of the model root chord. Forces normal and parallel to the root
chord and pitching moments were read on galvanometers or recorded on an
oscillograph with suitable low-pass filters to reduce the "hash" caused
by carriage vibration and cavitation.

It was necessary to install a number of seals as shown in figure 6
to minimize the effects of water circulating through the clearance gap
between the hydrofoil and the reflection plate and to keep water from
entering the balance. In addition, an air pressure of about $1\frac{1}{2}$ pounds
per square inch was maintained inside the balance housing to help oppose
the flow of water into the housing. Fouling contacts were located well
below the lowest set of strain gages in the balance so that they pro-
vided an indication when water entered the balance housing.

Before the tests the reflection plate was alined with the direction of motion by adjusting it until there was no change with speed of the static pressure measured at two orifices on the bottom surface of the plate. Underwater photographs of the plate indicated no cavitation on its bottom surface at any speed up to the maximum speed of the towing carriage.

A velocity survey made with a rake of total-pressure and static-pressure tubes mounted at the hydrofoil position showed that the reflection plate and its supporting fairing had negligible effect on the water speed below the plate. The rake was calibrated by towing it on a thin support below the water with only a small breaker plate to prevent air flowing down the sides of the support.

The thickness of the boundary layer under the reflection plate at the position of the hydrofoil root was measured at speeds of from 40 to 70 feet per second with a calibrated total-pressure tube of $\frac{1}{16}$-inch outside diameter and was found to be about 0.25 inch thick as shown in figure 7. As shown, this result agrees reasonably well with values computed for the thickness of turbulent boundary layers (ref. 2).

PROCEDURE

Test Procedure

The tests were made by setting the desired initial angle of attack α and taking readings of normal force, chordwise force, and pitching moment about the balance axis over a range of speeds starting at 20 feet per second. At speeds up to 60 feet per second, the forces and moments were read on galvanometers. At higher speeds, the internal damping and lag in the meters were too great to allow sufficient time for reading; therefore, the data were recorded on an oscillograph. The maximum speed at any angle of attack was the speed at which water entered the bottom of the balance housing, or the top speed of the towing carriage, 90 feet per second.

The appearance and extent of cavitation on the hydrofoils were determined by underwater pictures taken with a stationary 35-millimeter camera. Illumination was provided by high-intensity strobo-flash lamps under the water which were fired by the passage of the carriage.

The sweptback hydrofoils, especially the highly swept 60-4-0.6 hydrofoil, twisted under a load so that a washout was produced. The amount of twisting was approximated by applying normal force to the quarter-chord line at the spanwise stations of the centroids of the panels

inboard and outboard of the mean aerodynamic chord and measuring, for several values of normal force, the angular deflection at the mean aerodynamic chord and the tip chord with respect to the root of the hydrofoil. Figure 8 shows the twisting obtained from this loading on the three sweptback hydrofoils. The twist resulting at a given lift coefficient on the model hydrofoil would be the same as that which would occur on a full-size hydrofoil having the same modulus of elasticity operating at the same lift coefficient and speed. Also shown are the maximum lift loadings obtained during the tests of each swept hydrofoil.

Reduction of Data

The hydrofoils were tested with their spanwise direction perpendicular to the water surface and the towing gear had no measurable effect on the velocity at the hydrofoil position. No corrections were made for any possible surface effects or for any possible reduction in aspect ratio due to the finite extent of the reflection plate. The hydrofoils were so small relative to the cross-sectional area of the tank and relatively so far away from the walls that corrections for the closed channel were considered to be negligible.

The measured forces and moments were converted to lift, drag, and pitching moment about the quarter-mean-aerodynamic-chord point and these values were then put in coefficient form.

The pitching-moment data on all the hydrofoils except the 0-4-0.6 hydrofoil showed unexplained variations to the extent that its accuracy was suspected. Accordingly, pitching-moment data are given for the 0-4-0.6 hydrofoil only.

RESULTS AND DISCUSSION

Presentation of Results

The results of the tests are presented in the form of curves of lift coefficient, drag coefficient, and lift-drag ratio plotted against speed with angle of attack as a parameter in figures 9 to 12. A portion of the drag-coefficient plots has been shown to an enlarged scale in order to facilitate reading. The effects of speed on the hydrodynamic characteristics are shown in figures 13 to 16 in plots of angle of attack, drag coefficient, lift-drag ratio, and pitching-moment coefficient against lift coefficient. Typical cavitation pictures are presented in figures 17 to 20.

Although the hydrofoils were mounted with their spanwise axes per-
pendicular to the water surface, terms relating to lift, upper surface,
lower surface, and the like are used as though the hydrofoils were paral-
lel to the water surface with the lift acting upward. The angle of
attack of the hydrofoil root is referred to simply as angle of attack.

Effect of Cavitation on Hydrodynamic Characteristics

The principal effect of cavitation on the hydrodynamic character-
istics of the hydrofoils was to limit the maximum lift available to a
value of about 1900 to 2000 pounds per square foot, except for the
60-4-0.6 hydrofoil, which had a maximum lift of only 1210 pounds per
square foot. The maximum lift per square foot for hydrofoils other than
the 60-4-0.6 occurred when the upper surface of the hydrofoil was almost
completely covered by cavitation and was approximately equal to the dif-
ference between the free-stream static pressure and the vapor pressure
of the water. A similar value was observed in reference 3. For the
60-4-0.6 hydrofoil, the low value of the maximum lift attainable was
probably caused by the load-relieving effect of the large twisting indi-
cated by figure 8. Figure 11(a) indicates that the lift attainable
might be greater than 1210 pounds per square foot at angles of attack of
8° and less.

There were no large changes in the hydrodynamic characteristics
until a speed appreciably greater than the cavitation speed had been
reached, at which speed the cavitation had spread over an appreciable
portion of the hydrofoil. Similarly, airfoils do not necessarily experi-
ence marked changes in forces when passing through the critical speed.
As the speed increased above cavitation speed, the cavitation spread over
a greater portion of the hydrofoil and the lift coefficient at constant
angle of attack generally increased somewhat and then decreased again to
meet and follow the curve of maximum lift available. The drag coeffi-
cient followed much the same trend but in such a manner that the lift-
drag ratio generally tended to decrease with increase in speed.

The effect of cavitation on the pitching-moment characteristics is
illustrated in figure 9(d). Increasing the speed in the cavitating
region increased the cavitation area and produced a rather rapid nose-
down change in pitching-moment coefficient (rearward shift of the center
of pressure) of the unswept 0-4-0.6 hydrofoil at constant angles of
attack. This effect has been observed on airfoils passing through criti-
cal speed. As the speed for any angle of attack approached that corre-
sponding to the maximum lift available, the rearward shift of the center
of pressure ceased and then reversed and moved the center of pressure
back towards the leading edge. This change agrees with the variation
obtained by considering the spread of cavitation over the surface of a
hydrofoil section to be equivalent to cutting off the peak of the

upper-surface pressure distribution at the value of the vapor pressure
of water. As the speed increases more of the peak is cut off and the
increasing contribution of the pressure towards the trailing edge moves
the center of pressure rearward. When the upper-surface pressure is at
the vapor pressure over the complete chord (section completely covered
by cavitation or condition of maximum lift available), the center of
pressure is approximately at the 50-percent-chord station as the lift
would probably be provided mainly by the upper-surface pressure distri-
bution, at least, until speeds greater than those of the present tests
are reached. The pressure distribution over the lower surface will, of
course, be changed from its original shape by the change of shape of the
upper-surface pressure distribution.

Effect of Sweep on Cavitation and Force Characteristics

Cavitation on the unswept 0-4-0.6 hydrofoil first formed in a narrow
band near the leading edge, and extended farther chordwise with increasing
speed (fig. 17). Cavitation on the swept hydrofoils, at high angles of
attack, however, (figs. 18 and 19) spread out from a point at the root
leading edge and had the general appearance of the vortex flow shown dia-
grammatically in figures 5(c) and 5(d) of reference 4. This type of flow
was more pronounced for the highly swept 60-4-0.6 hydrofoil than for the
45-4-0.6 hydrofoil. At low angles of attack, the cavitation on the swept
hydrofoils started approximately at the leading edge and progressed to an
appearance intermediate between that of vortex flow and that of the
unswept hydrofoil.

The theoretical cavitation speed of the 0-4-0.6 hydrofoil was com-
puted from the theoretical pressure distribution for the 65A006 section
given in reference 5 by using the relation

$$V_c = \sqrt{\frac{2(p_0 - p_v)}{\rho(S_{max} - 1)}}$$

The ratio of the peak local section lift coefficient to the average lift
coefficient was determined from reference 6. This ratio made the hydro-
foil cavitation speed about two feet per second less than that for uni-
form spanwise lift distribution. The actual cavitation speed of the
hydrofoil agreed with the theoretical speed up to a lift coefficient of
about 0.25 but was greater than the theoretical at greater lift coeffi-
cients (fig. 21). This result indicates that at lift coefficients
greater than 0.25, the negative pressure on the upper surface of the
hydrofoil was less than that predicted by theory. A similar collapse of
the pressure peak and the appearance of a region of approximately

constant pressure on the NACA 64A006 airfoil section was noted in refer-
ence 7 and was shown to be caused by boundary-layer separation.

Cavitation speeds of the NACA 64A006 airfoil section computed from
the theoretical pressure distributions of reference 5 and from the experi-
mental pressure distribution of reference 7 are compared in figure 22.
It can be seen that they follow the same trends as do the theoretical
and experimental cavitation speeds of the 0-4-0.6 hydrofoil having the
65A006 airfoil section (fig. 21).

Figure 21 shows the effect of sweep on the observed and calculated
cavitation speeds on a basis of lift coefficient. The calculated cavi-
tation speeds for the swept hydrofoils were obtained from the calculated
values for the unswept hydrofoil by using the method of reference 8. It
can be seen that the observed cavitation speed of the 45-4-0.6 hydrofoil
was generally greater than that of the 0-4-0.6 hydrofoil. The observed
cavitation speed of the 60-4-0.6 hydrofoil was not much different than
that of the 45-4-0.6 hydrofoil. The same is true of the calculated cavi-
tation speeds for these two hydrofoils. Throughout the range of lift
coefficients investigated for the swept hydrofoils, the observed values
of cavitation speed were greater than the calculated values. This dif-
ference is attributed to the boundary-layer-separation phenomenon pre-
viously mentioned.

Figure 23 compares the hydrodynamic force characteristics of the
hydrofoils with 0°, 45°, and 60° sweepback. It can be seen that, through-
out the entire speed range, increasing the angle of sweep results in a
deterioration of lift coefficient with increasing speed and an increase
in induced drag coefficient with increasing lift coefficient. The effect
of sweep on lift-drag ratio in both the noncavitating and the cavitating
conditions is shown in figure 24. At lift coefficients below 0.2 there
is little decrease in efficiency to 45° of sweepback. At greater lift
coefficients and greater angles of sweepback there was a large decrease
in lift-drag ratio. These effects are similar to those observed on swept
wings (ref. 1).

Effect of Taper Ratio on Cavitation and

Force Characteristics

The cavitation speeds of the 45-4-0.6 and 45-4-0.3 hydrofoils are
shown in figure 25. The more highly tapered hydrofoil had slightly
greater cavitation speeds than the 45-4-0.6 hydrofoil and displayed the
same tendency for the cavitation speed to be higher than the theoretical
cavitation speed.

Figure 26 compares the hydrodynamic force characteristics of the 45° swept hydrofoil with different taper ratios. It is apparent that the characteristics were not greatly affected by the change in taper ratio, either in the cavitating or the noncavitating range. The small magnitude of the effect of the change in taper ratio on the efficiency of the hydrofoil is shown in figure 27.

Comparison with Wind-Tunnel Data

Hydrodynamic force and moment characteristics of the hydrofoils at a subcavitation speed (Reynolds number of 0.5×10^6) are compared with low-speed aerodynamic characteristics at fairly large Reynolds numbers and with aerodynamic characteristics at low Reynolds numbers and low subsonic Mach numbers in figure 28. The aerodynamic characteristics were obtained from references 1, 9, and 10, and from the wing-alone wall data presented in reference 11.

Although there was a small amount of cavitation on the hydrofoils at the higher lift coefficients for the speed under consideration, figures 9 to 12 show that it had a negligible effect on the hydrodynamic characteristics, except possibly at the stall; therefore, the hydrodynamic characteristics of figure 28 may be considered representative of subcavitation characteristics.

In general, the hydrofoils at a Reynolds number of 0.5×10^6 had lower slope of the lift curve, greater induced drag, and lower lift coefficient for the pitching-moment break than the wings. This result may be due to an aspect-ratio reduction resulting from the finite extent of the reflection plate. The differences in lift-curve slope are in qualitative agreement with the separate effects of Reynolds number and Mach number on lift-curve slope. The lift coefficient at which the pitching moment broke would be expected to be lower at low Reynolds numbers than at high Reynolds numbers (ref. 1).

CONCLUSIONS

The results of an investigation to determine the effects of sweepback and taper ratio on the cavitation and hydrodynamic force and pitching-moment characteristics of semispan hydrofoils having an aspect ratio of 4 and NACA 65A006 airfoil sections led to the following conclusions:

1. Increasing the sweepback of the hydrofoils from 0° to 45° resulted in an increase in cavitation speed, but a further increase to

60° of sweep gave little or no additional increase. For these hydrofoils, sweepback decreased lift-drag ratios both in the cavitating and noncavitating conditions.

2. The twist occurring on the hydrofoil with 60° of sweepback was sufficient to obscure the effect of its angle of sweep. This twist was great enough to limit the maximum lift of the 60° swept hydrofoil to 1210 pounds per square foot, whereas the corresponding values for the 0° and 45° sweptback hydrofoils were 2050 and 1900 pounds per square foot, respectively.

3. A change in taper ratio from 0.6 to 0.3 on a hydrofoil with 45° of sweepback resulted in only negligible effects on the cavitation speed and the force characteristics.

4. The cavitation speed of the unswept hydrofoil at moderate and high lift coefficients was higher than that computed from theoretical pressure distributions, probably because of boundary-layer separation. The variation of cavitation speed with lift coefficient of the swept hydrofoils was similar to that of the unswept hydrofoil.

5. The hydrodynamic characteristics of the hydrofoils at subcavitation speeds were in reasonable agreement with the aerodynamic characteristics of similar wings, and the effects of sweep and taper on the subcavitation hydrodynamic characteristics were approximately the same as for wings.

Langley Aeronautical Laboratory,
    National Advisory Committee for Aeronautics,
        Langley Field, Va.

REFERENCES

1. Cahill, Jones F., and Gottlieb, Stanley M.: Low-Speed Aerodynamic
     Characteristics of a Series of Swept Wings Having NACA 65A006 Air-
     foil Sections (Revised). NACA RM L50F16, 1950.

2. Dodge, Russell A., and Thompson, Milton J.: Fluid Mechanics.
     First ed., McGraw-Hill Book Co., Inc., 1937, p. 324.

3. Benson, James M., and Land, Norman S.: An Investigation of Hydro-
     foils in the NACA Tank. I - Effect of Dihedral and Depth of Sub-
     mersion. NACA ACR, Sept. 1942.

4. Wilson, Herbert A., Jr., and Lovell, J. Calvin: Full-Scale Investi-
     gation of the Maximum Lift and Flow Characteristics of an Airplane
     Having Approximately Triangular Plan Form. NACA RM L6K20, 1947.

5. Loftin, Laurence K., Jr.: Theoretical and Experimental Data for a
     Number of NACA 6A-Series Airfoil Sections. NACA Rep. 903, 1948.
     (Supersedes NACA TN 1368.)

6. DeYoung, John: Theoretical Additional Span Loading Characteristics
     of Wings With Arbitrary Sweep, Aspect Ratio, and Taper Ratio.
     NACA TN 1491, 1947.

7. McCullough, George B., and Gault, Donald E.: Boundary-Layer and
     Stalling Characteristics of the NACA 64A006 Airfoil Section. NACA
     TN 1923, 1949.

8. Neumark, S.: Critical Mach Numbers for Thin Untapered Swept Wings
     at Zero Incidence. Rep. No. Aero 2355, British R.A.E., Nov. 1949.

9. King, Thomas J., Jr., and Myers, Boyd C., II: Aerodynamic Character-
     istics of a Wing With Quarter-Chord Line Swept Back 60°, Aspect
     Ratio 4, Taper Ratio 0.6, and NACA 65A006 Airfoil Section.
     Transonic-Bump Method. NACA RM L9G27, 1949.

10. Spreemann, Kenneth P., and Alford, William J., Jr.: Small-Scale
     Investigation at Transonic Speeds of the Effects of Thickening the
     Inboard Section of a 45° Sweptback Wing of Aspect Ratio 4, Taper
     Ratio 0.3, and an NACA 65A006 Airfoil Section. NACA RM L51F08a,
     1951.

11. Donlan, Charles J., Myers, Boyd C., II, and Mattson, Axel T.: A
     Comparison of the Aerodynamic Characteristics at Transonic Speeds
     of Four Wing-Fuselage Configurations as Determined From Different
     Test Techniques. NACA RM L50H02, 1950.

TABLE I

ORDINATES OF NACA 65A006 HYDROFOIL SECTION
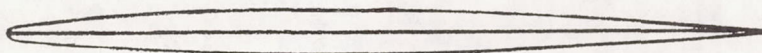
Station, percent c	Ordinate, percent c
0	0
.5	.464
.75	.563
1.25	.718
2.5	.981
5.0	1.313
7.5	1.591
10	1.824
15	2.194
20	2.474
25	2.687
30	2.842
35	2.945
40	2.996
45	2.992
50	2.925
55	2.793
60	2.602
65	2.364
70	2.087
75	1.775
80	1.437
85	1.083
90	.727
95	.370
100	.013

L.E. radius: 0.229 percent c

T.E. radius: 0.014 percent c
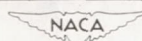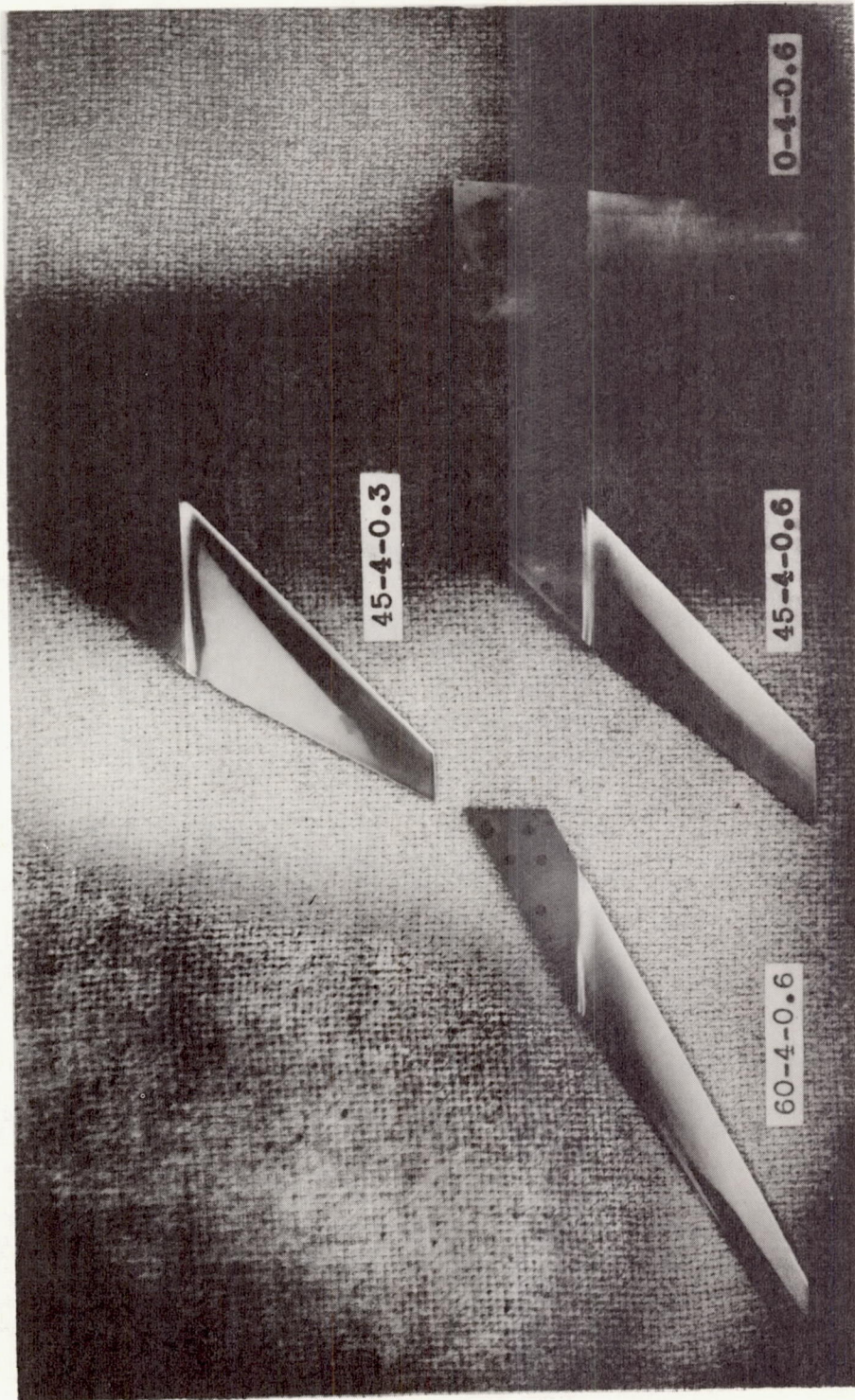
Figure 1.- Semispan hydrofoils.   L-76955
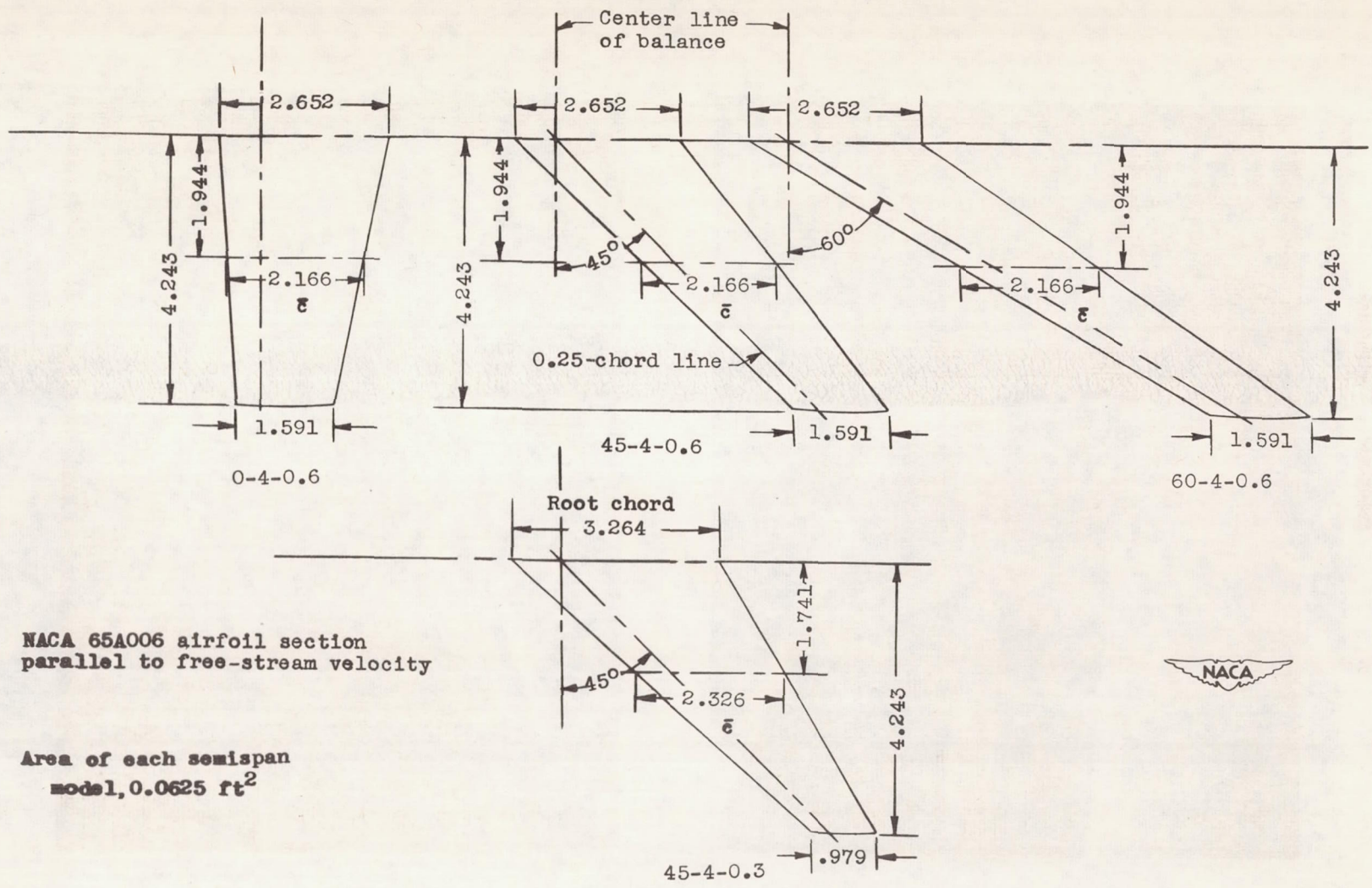
Figure 2.- Dimensions of semispan hydrofoils. All dimensions are in inches.

Figure 3.- Towing gear.

Support
frame

Balance
housing

Water
surface

Reflection plate

Hydrofoil

0   6   12
Scale, inches
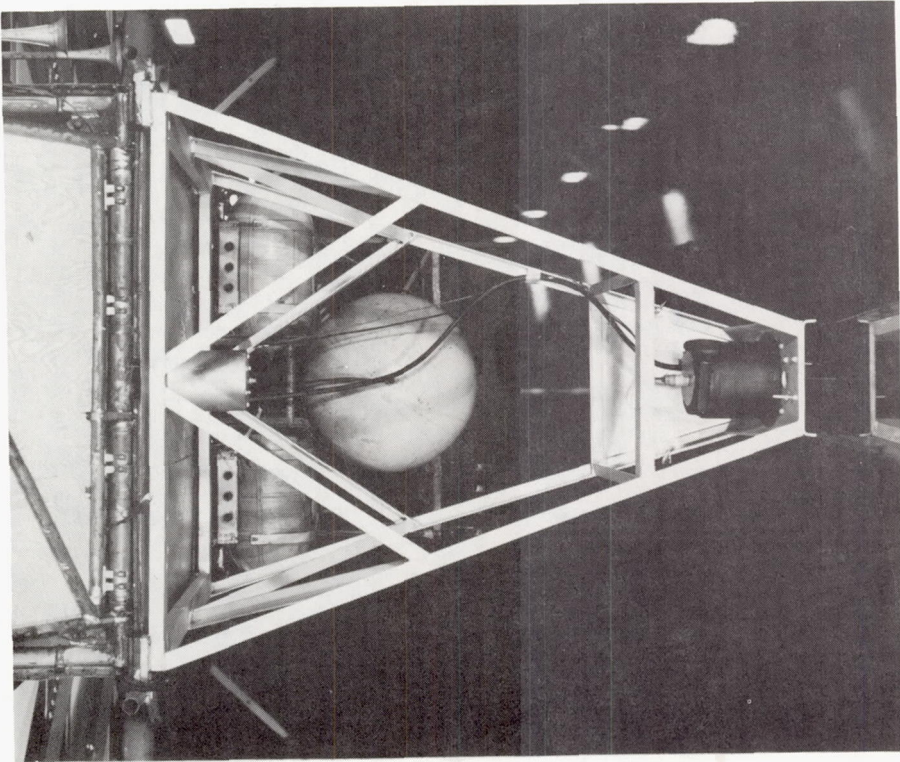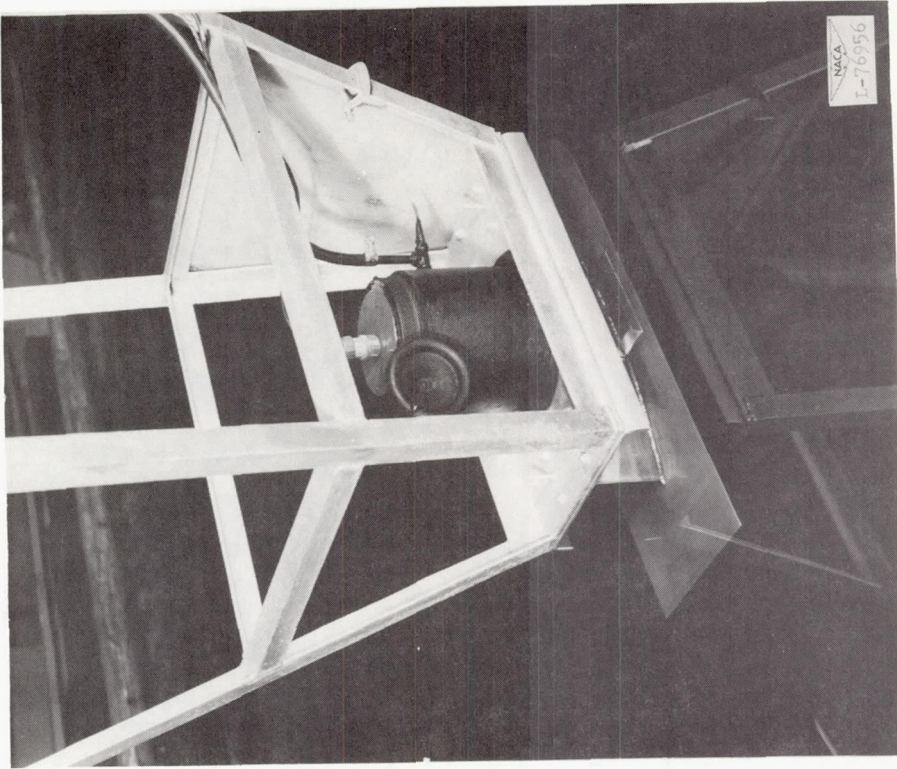
NACA
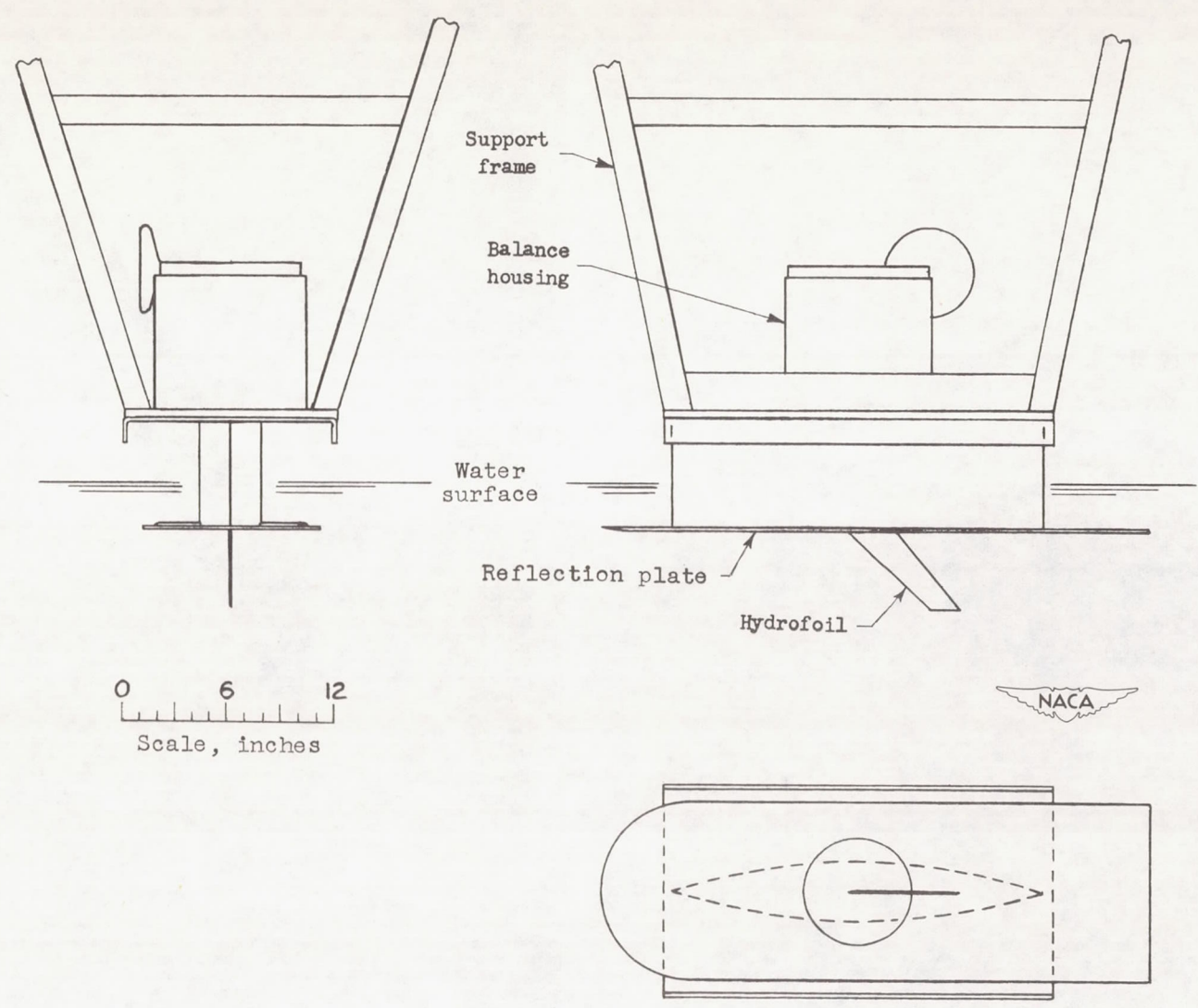
Figure 4.- Sketch of towing gear.
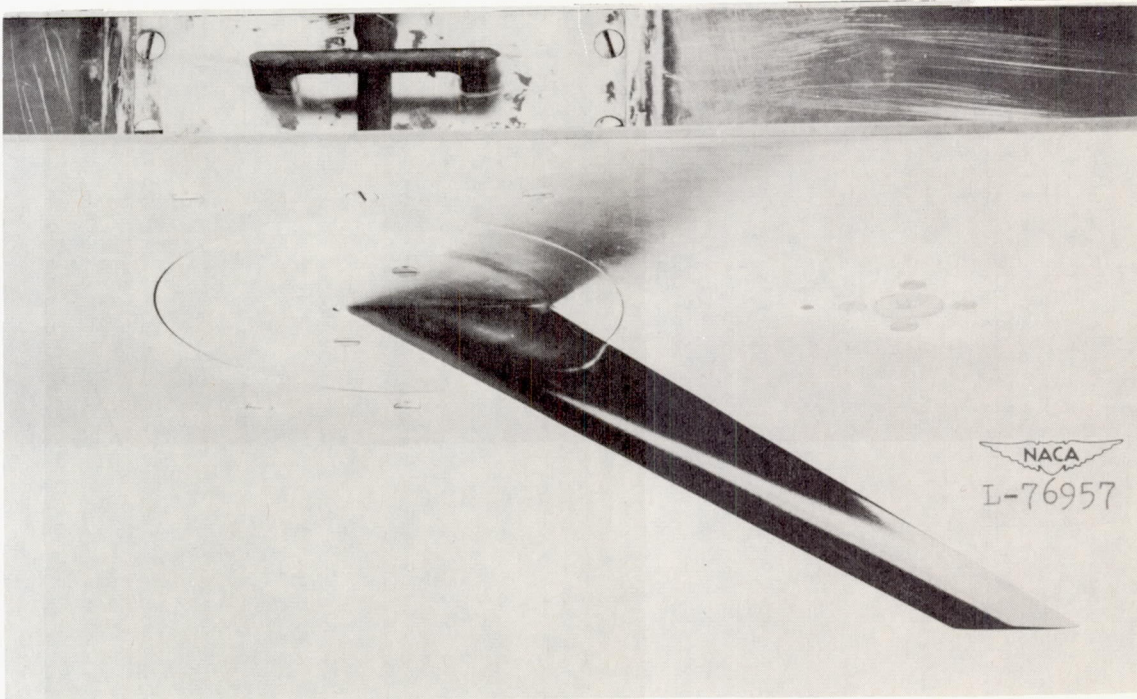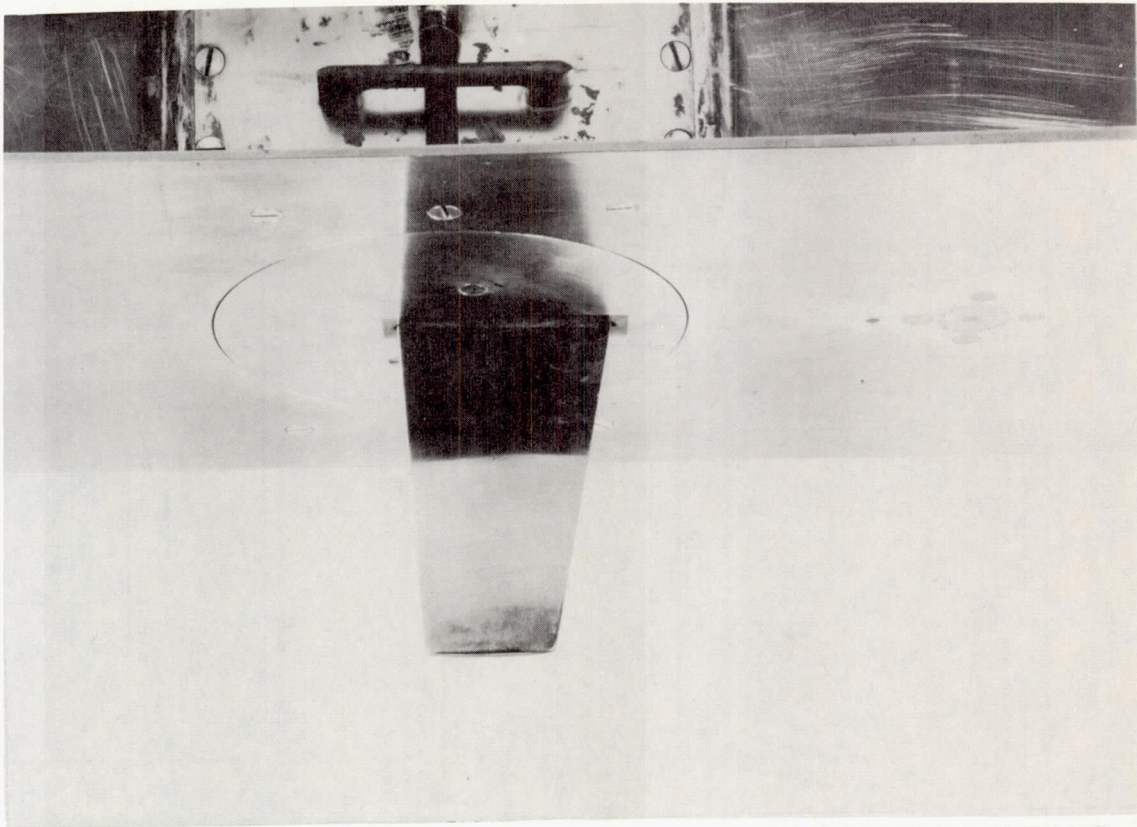
Figure 5.- The 0-4-0.6 and 60-4-0.6 hydrofoils mounted on the towing gear.

Balance housing

Balance staff

Flat rubber ring

Flexible rubber tube
cemented in position

Clearance gap

Sponge rubber
cemented in position

Hydrofoil

0   1   2
Scale, inches

NACA
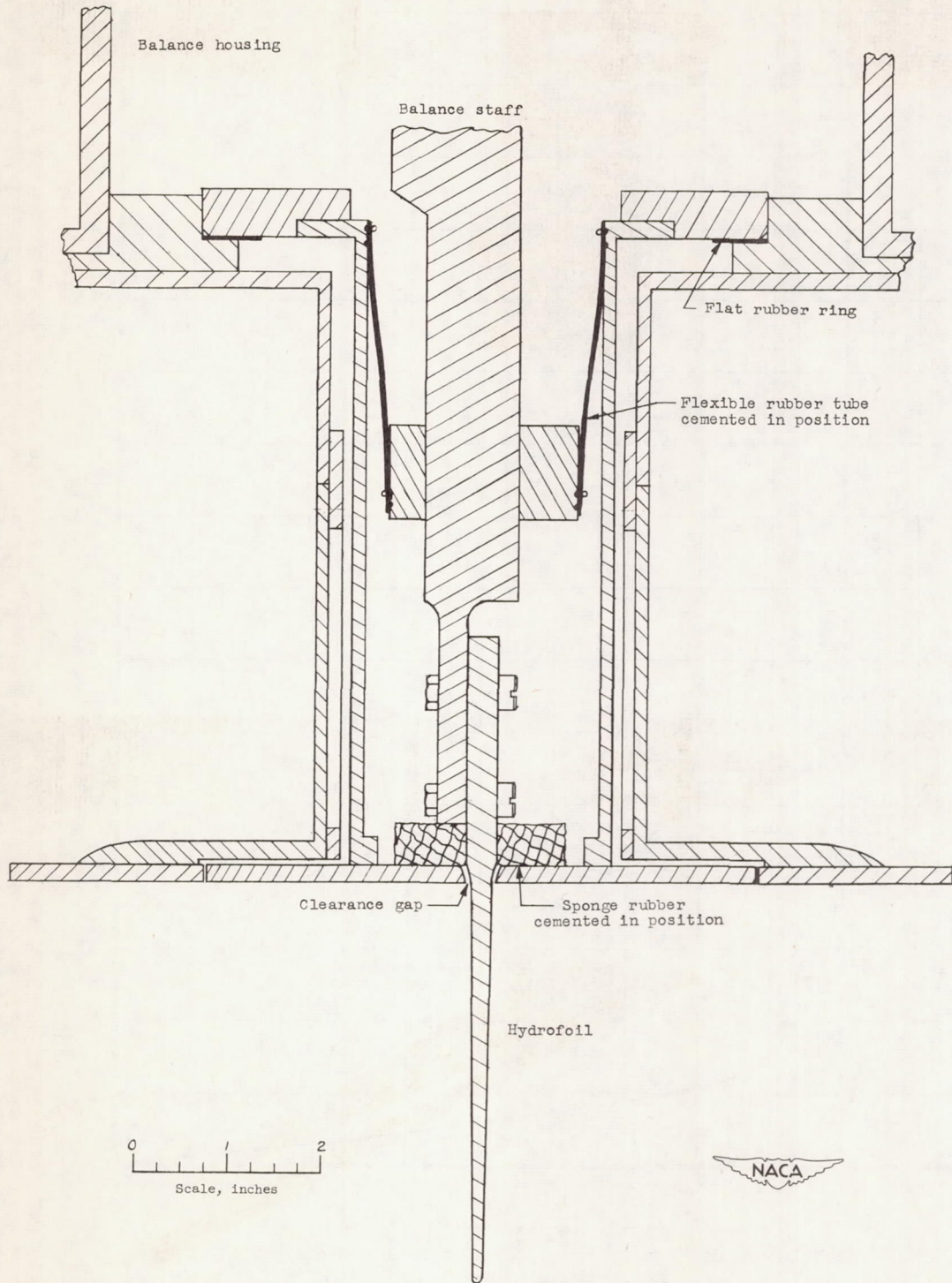
Figure 6.- Cross-sectional view of towing gear showing seals.
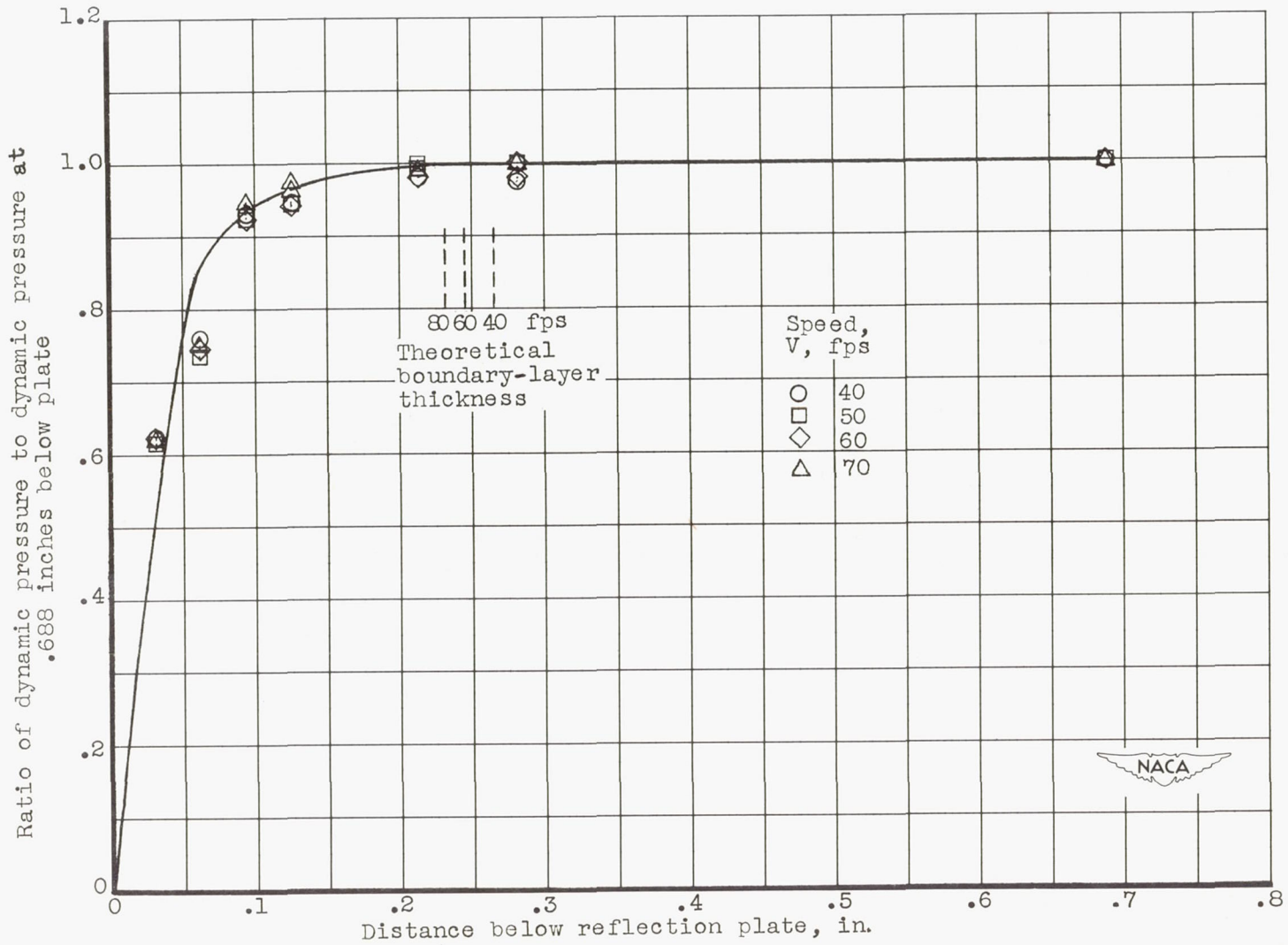
Figure 7.- Boundary-layer thickness on reflection plate at hydrofoil position.
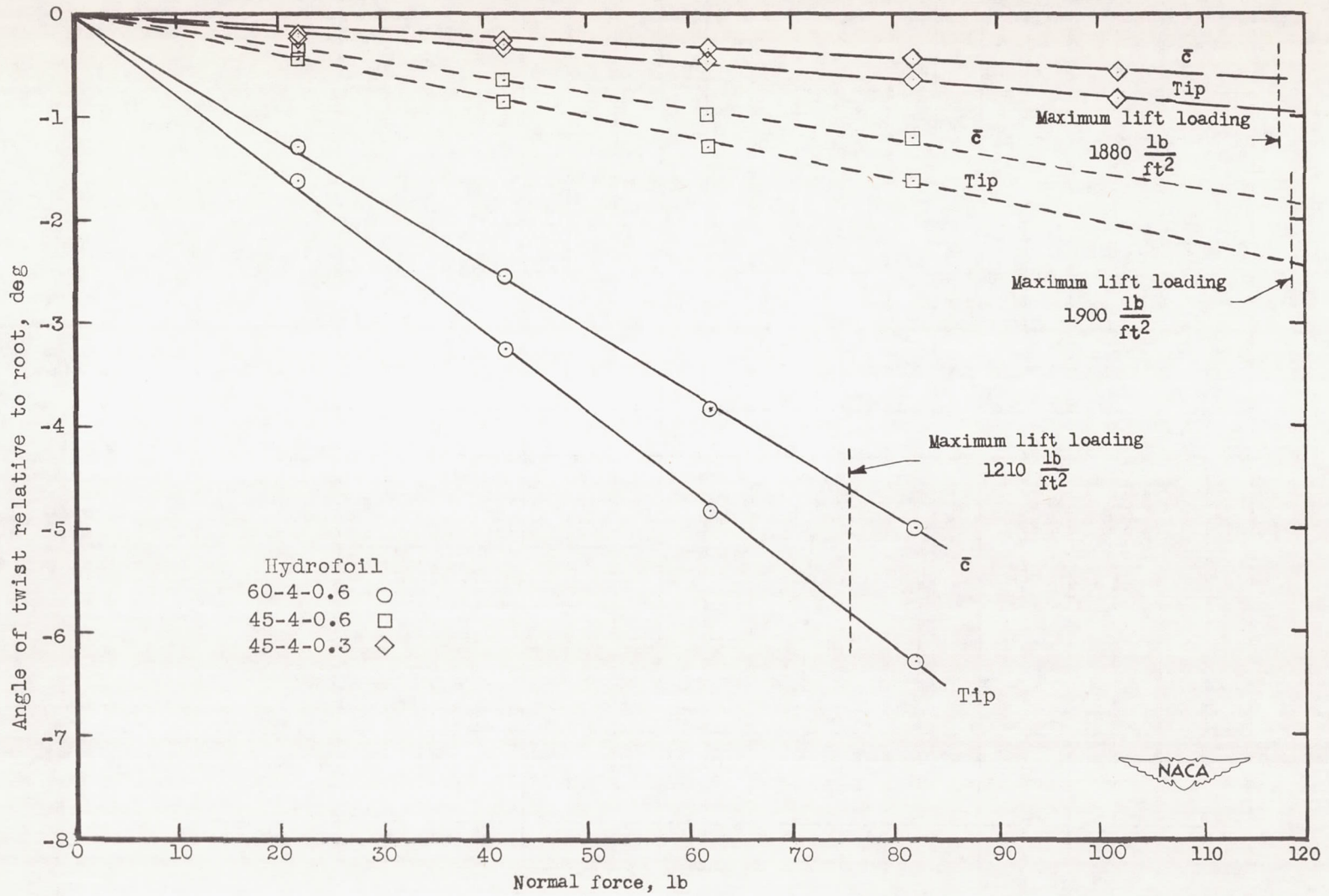
Figure 8.- Angular deflection of sweptback hydrofoils due to load.
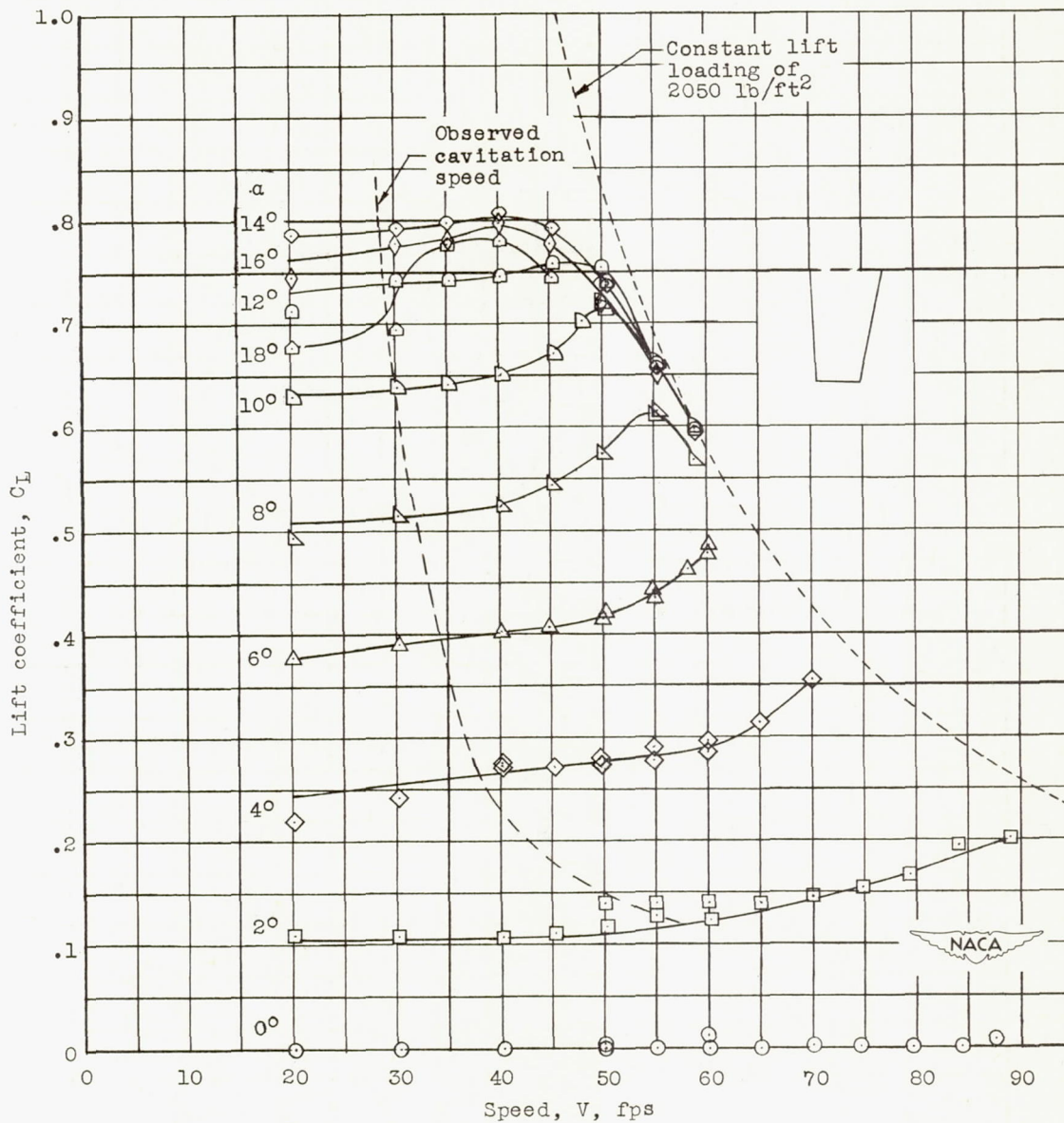
(a) Lift coefficient.

Figure 9.- Variation with speed of hydrodynamic characteristics
of 0-4-0.6 hydrofoil.
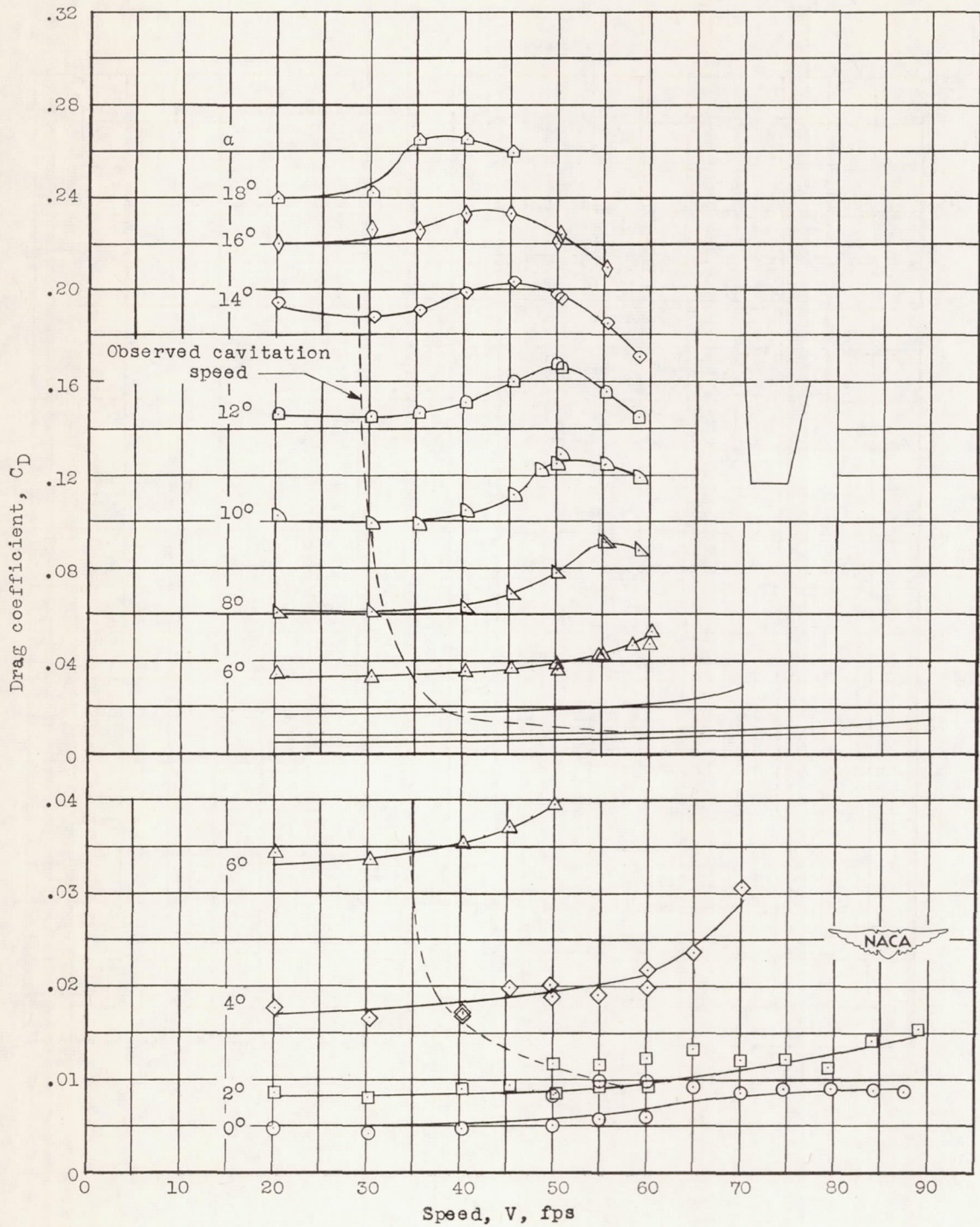
(b) Drag coefficient.

Figure 9.- Continued.
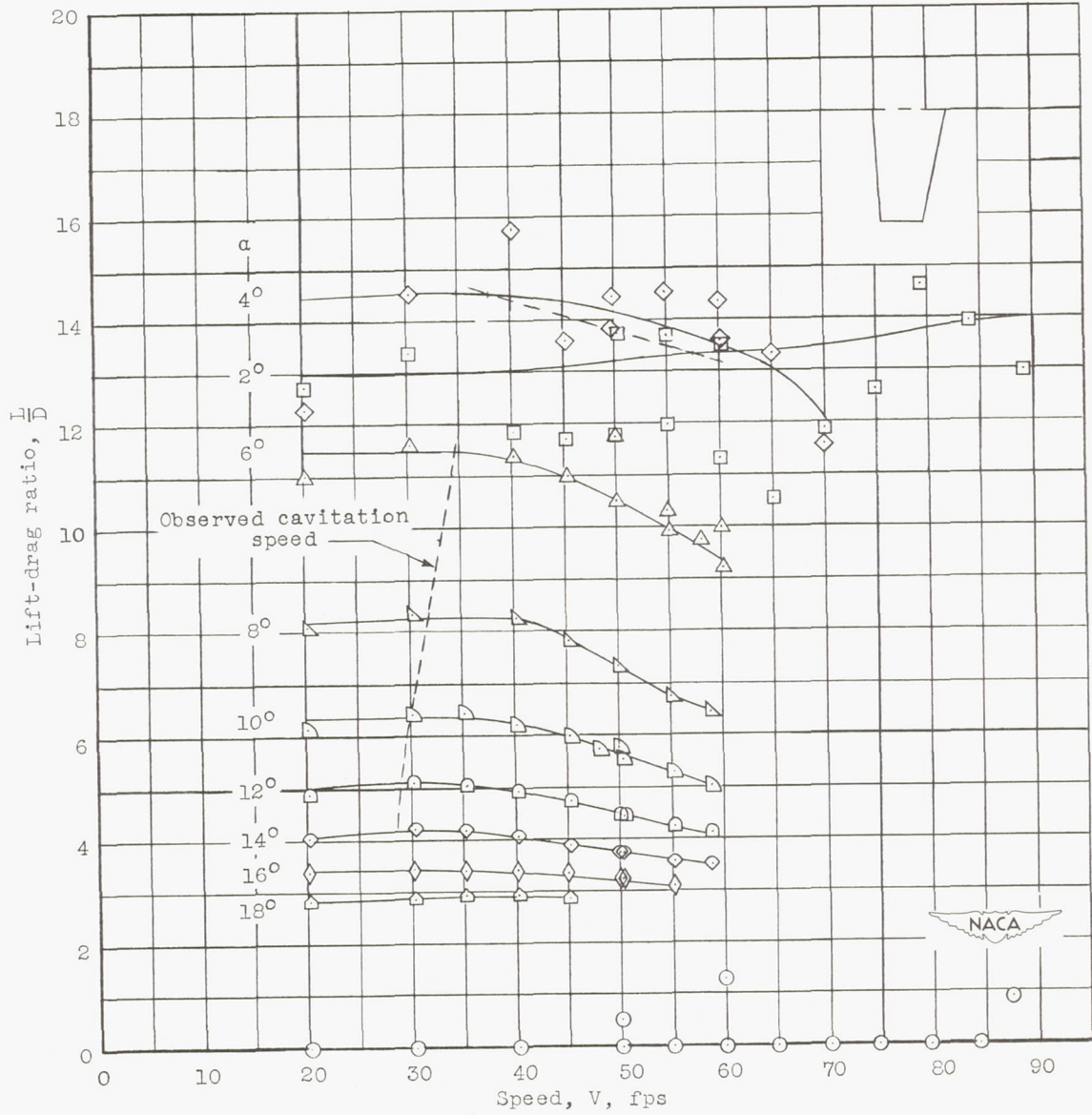
(c) Lift-drag ratio.

Figure 9.- Continued.
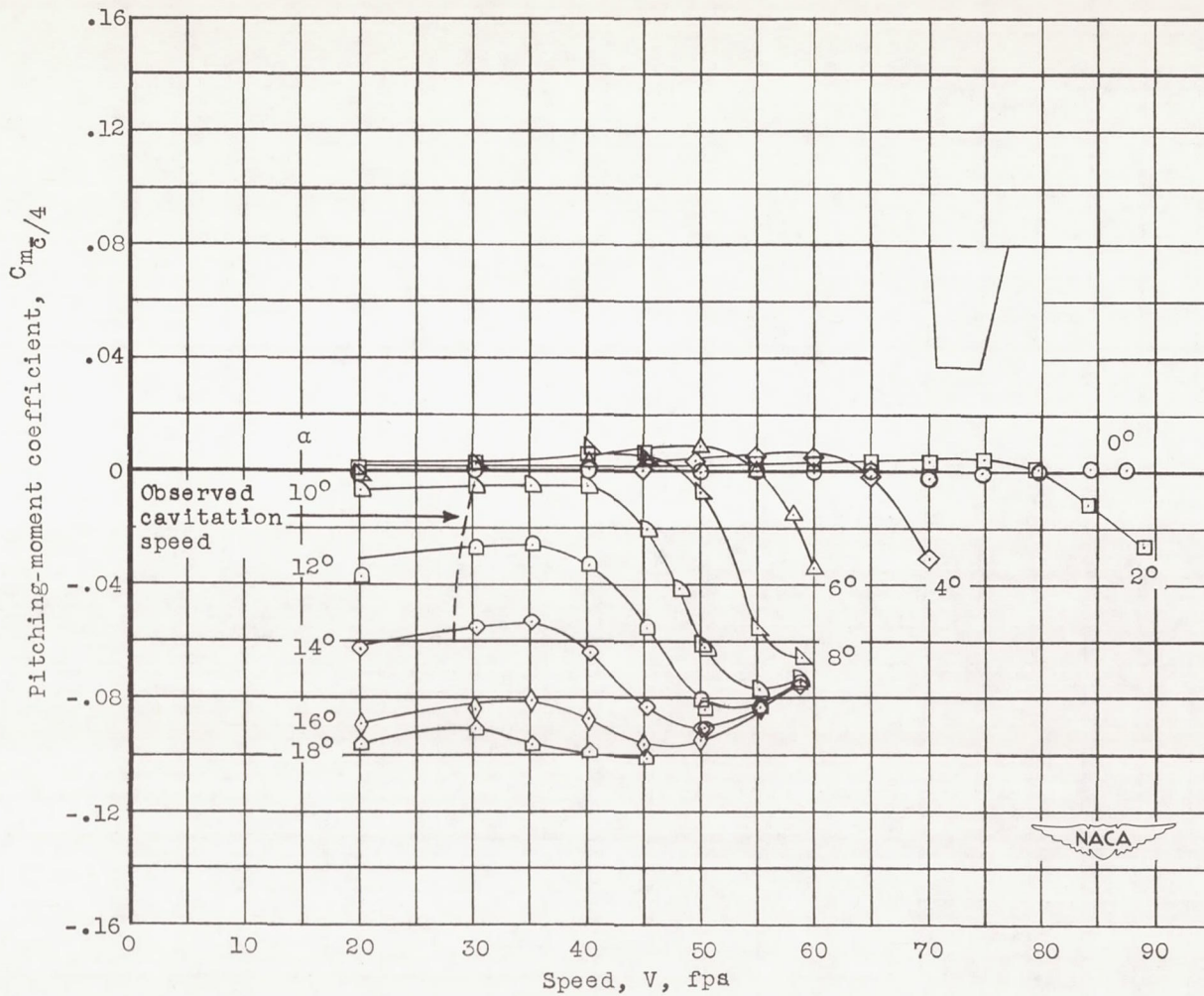
(d) Pitching-moment coefficient.

Figure 9.- Concluded.
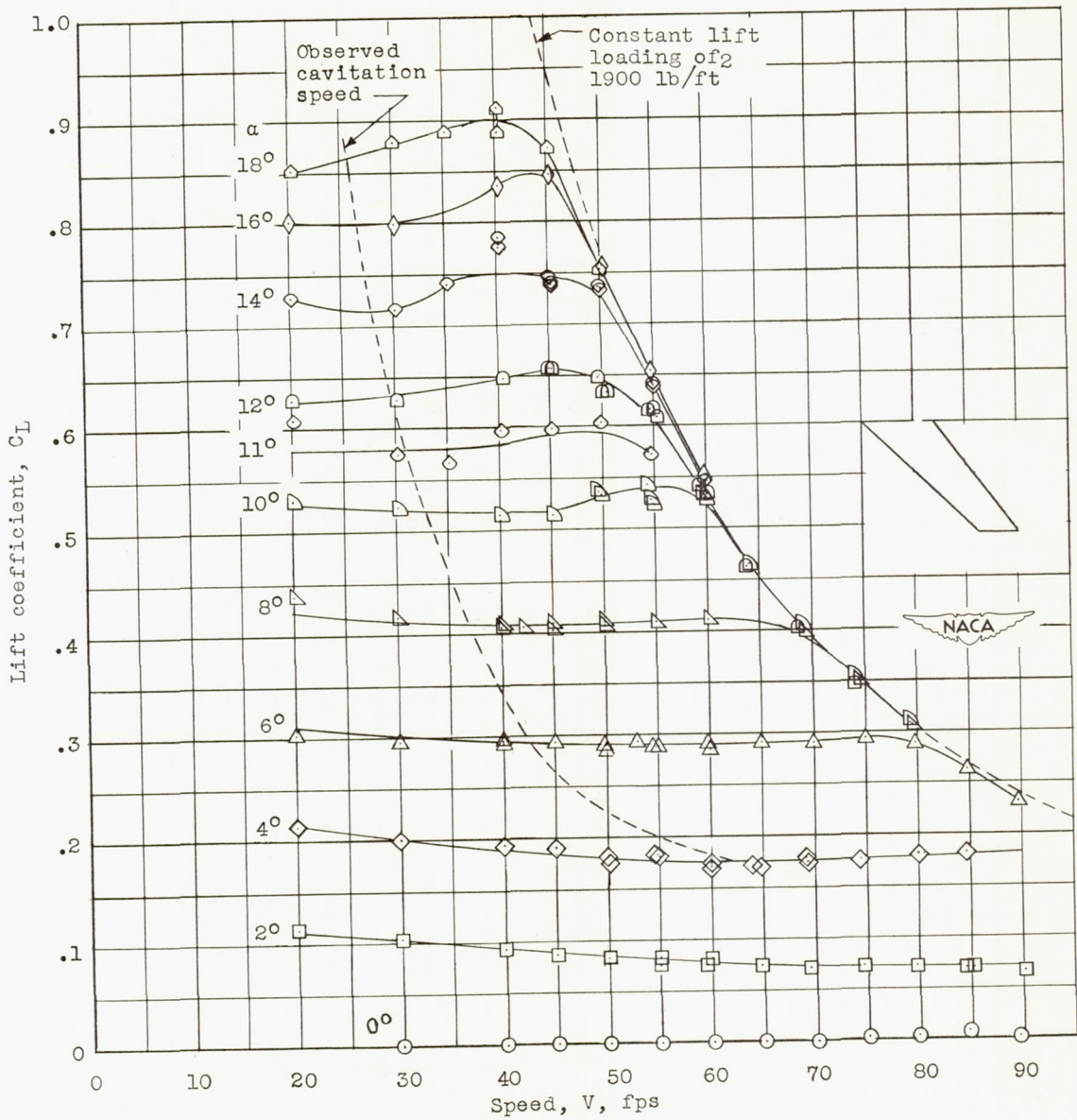
(a) Lift coefficient.

Figure 10.- Variation with speed of hydrodynamic characteristics
of 45-4-0.6 hydrofoil.
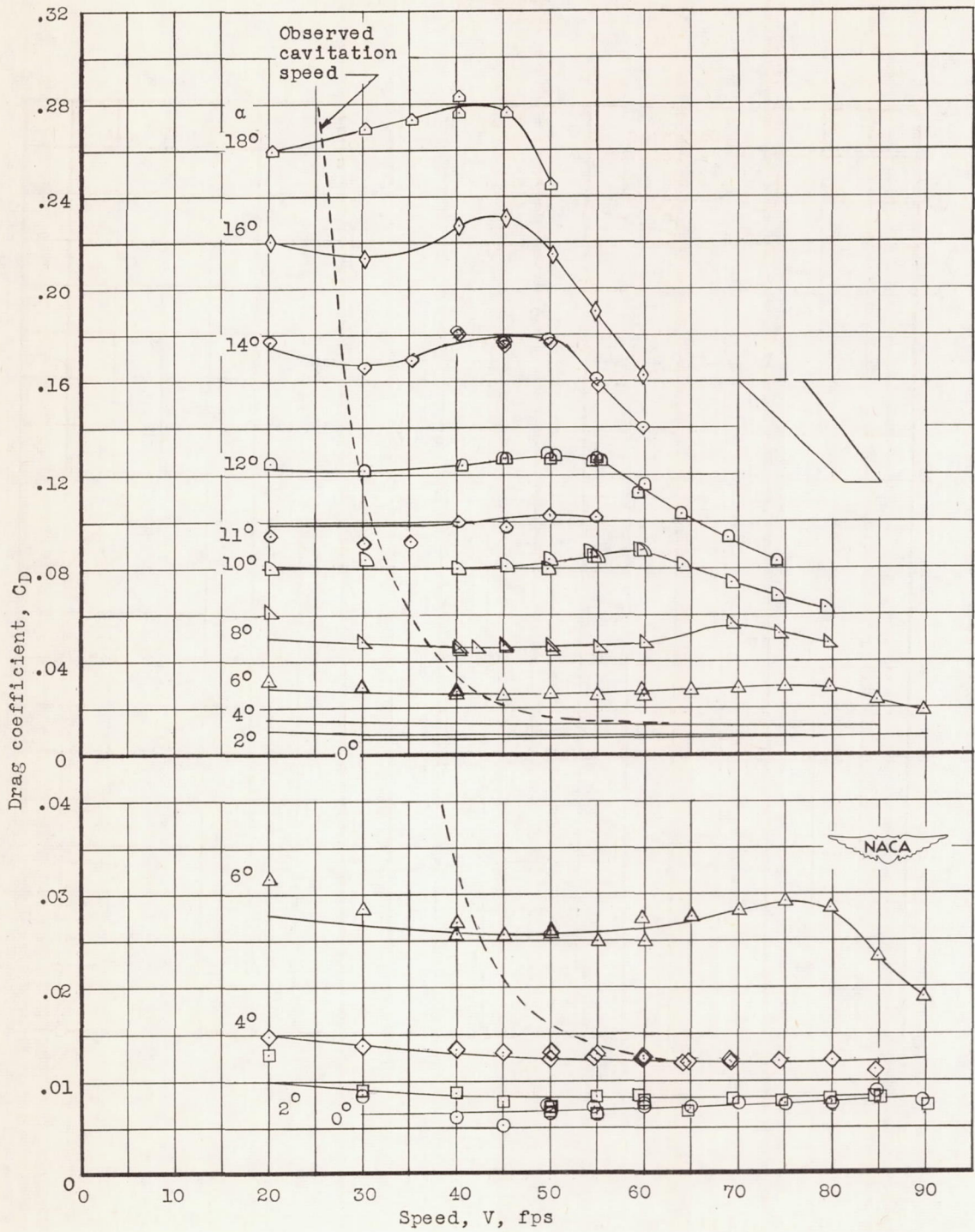
(b) Drag coefficient.

Figure 10.- Continued.
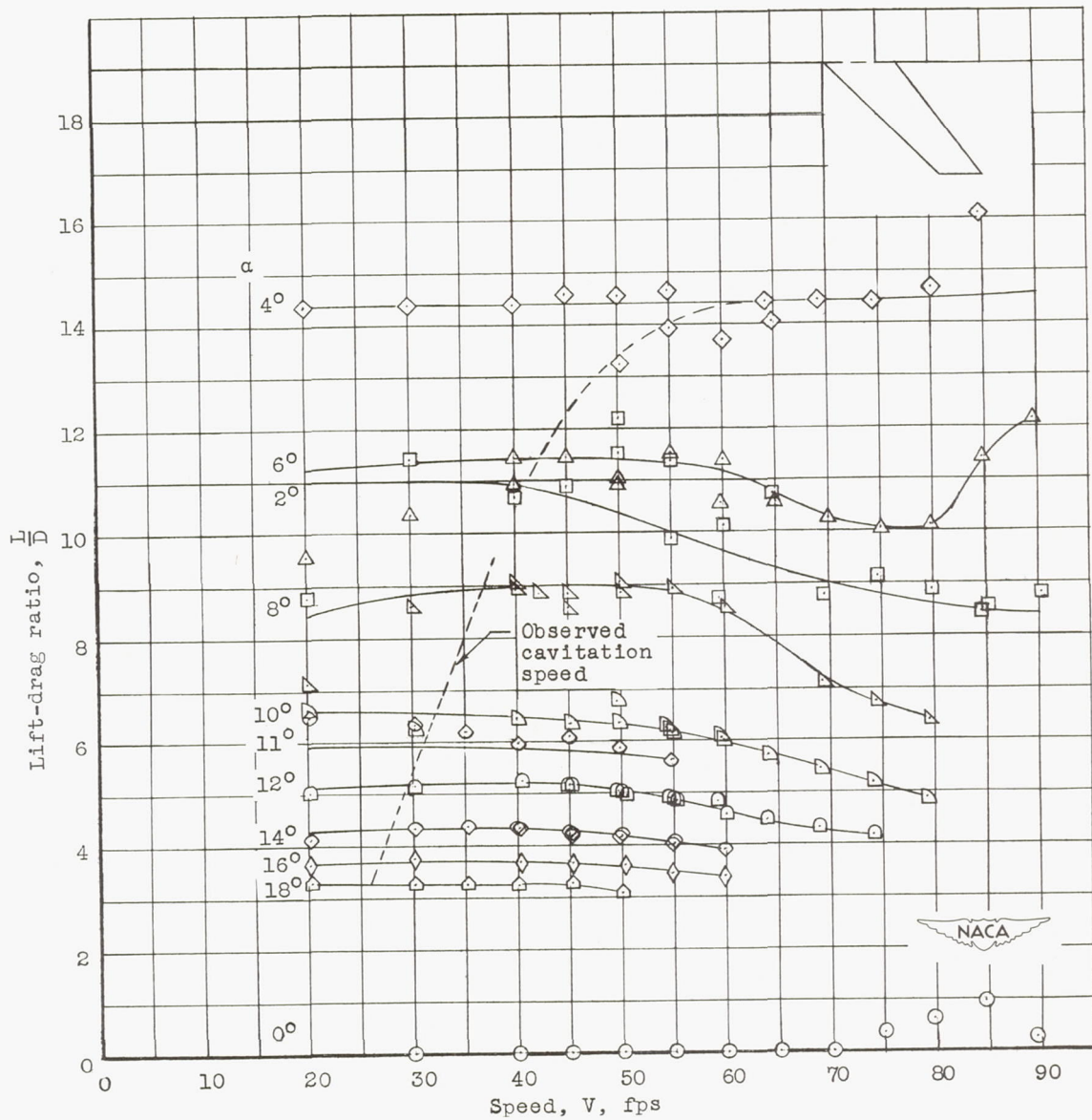
(c) Lift-drag ratio.

Figure 10.- Concluded.
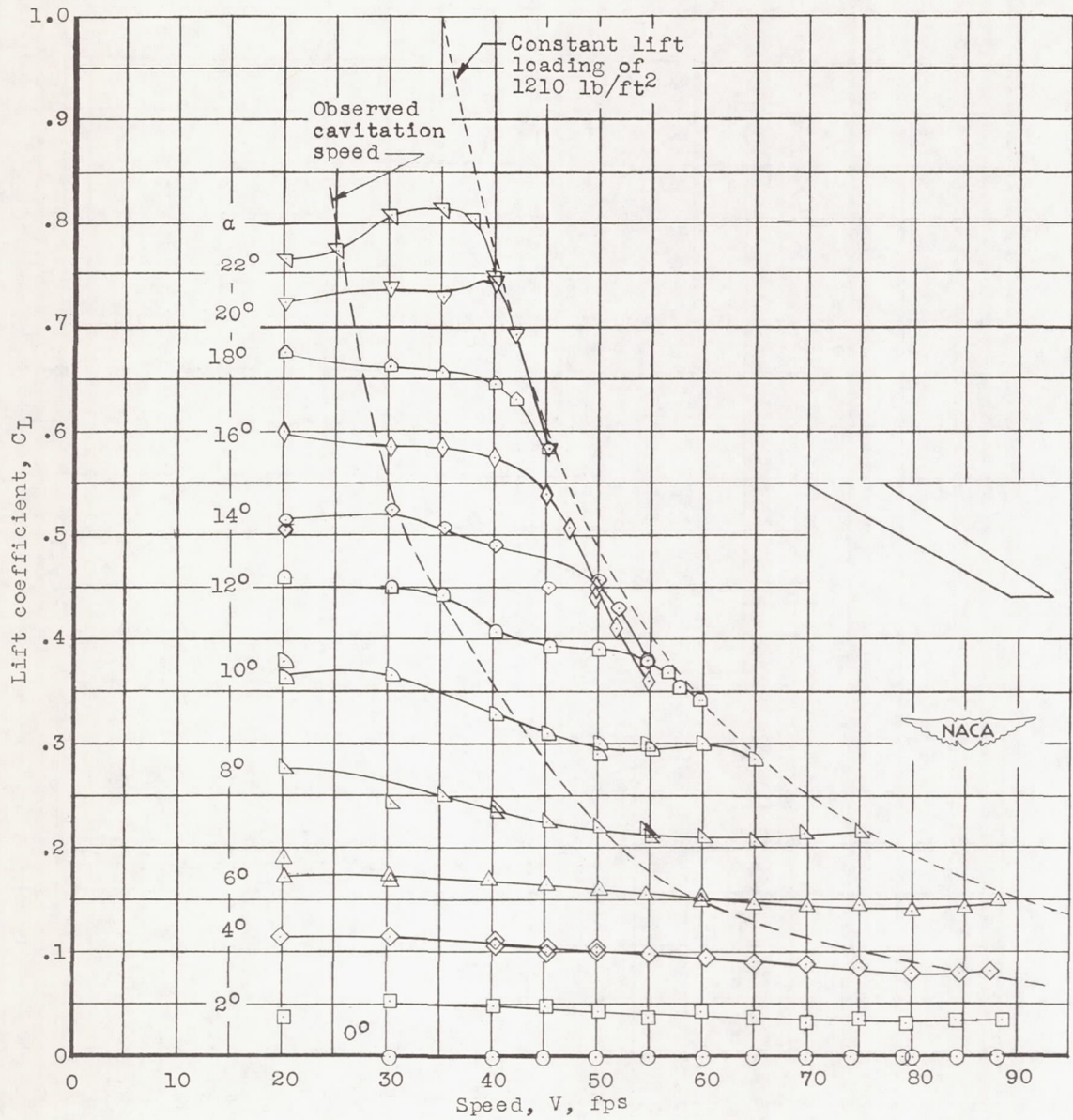
(a) Lift coefficient.

Figure 11.- Variation with speed of hydrodynamic characteristics
of 60-4-0.6 hydrofoil.
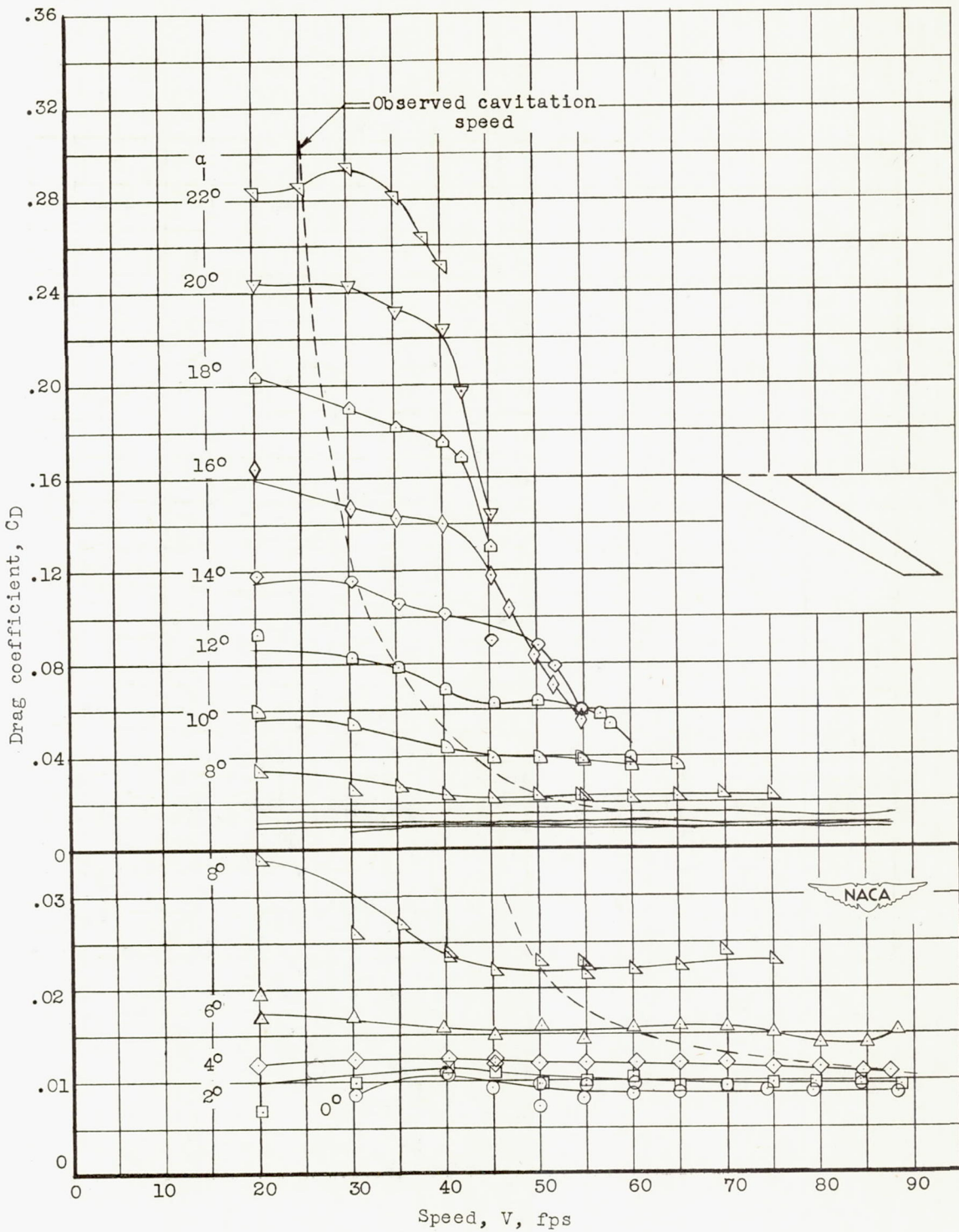
(b) Drag coefficient.

Figure 11.- Continued.
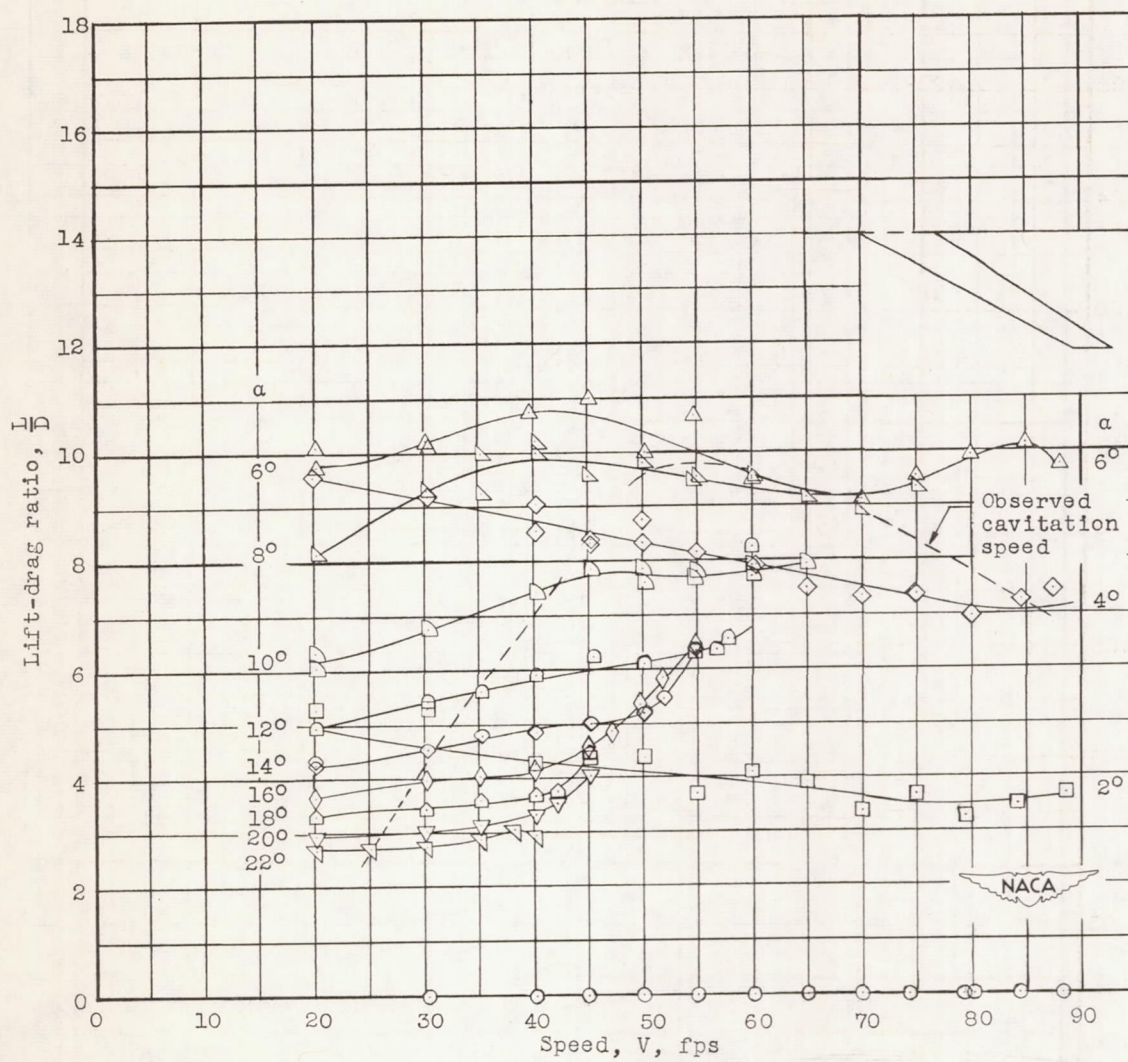
(c) Lift-drag ratio.

Figure 11.- Concluded.
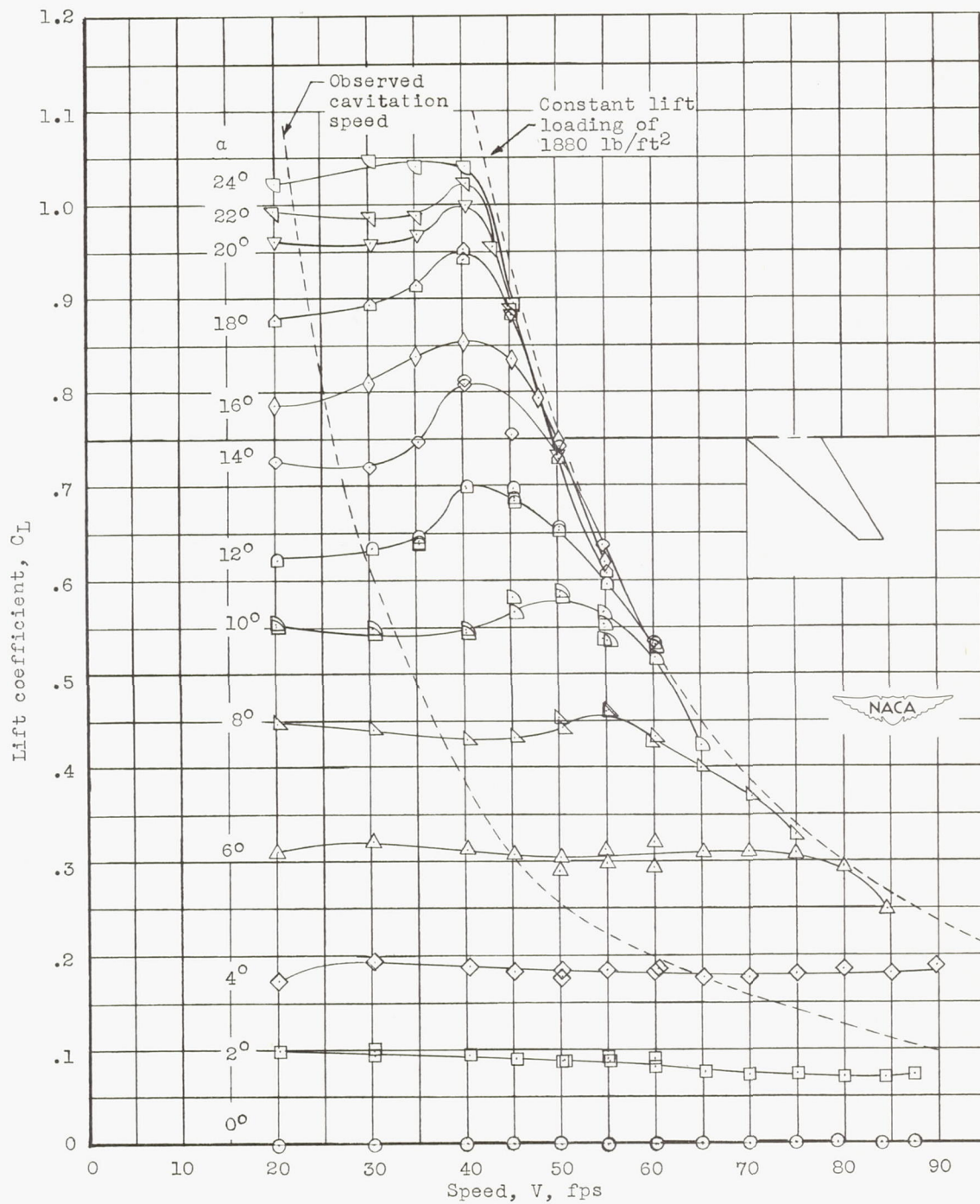
(a) Lift coefficient.

Figure 12.- Variation with speed of hydrodynamic characteristics
of 45-4-0.3 hydrofoil.
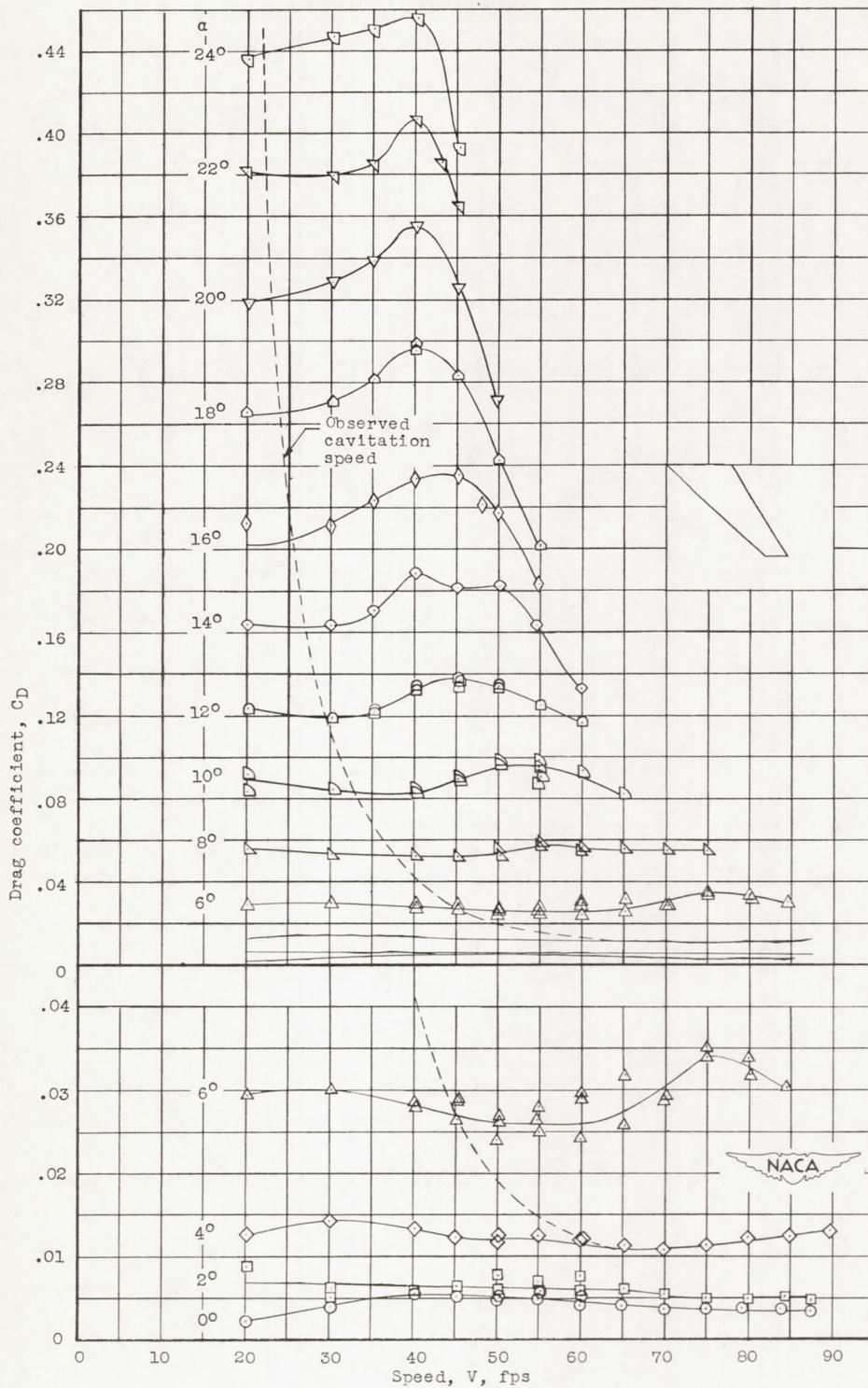
(b) Drag coefficient.

Figure 12.- Continued.
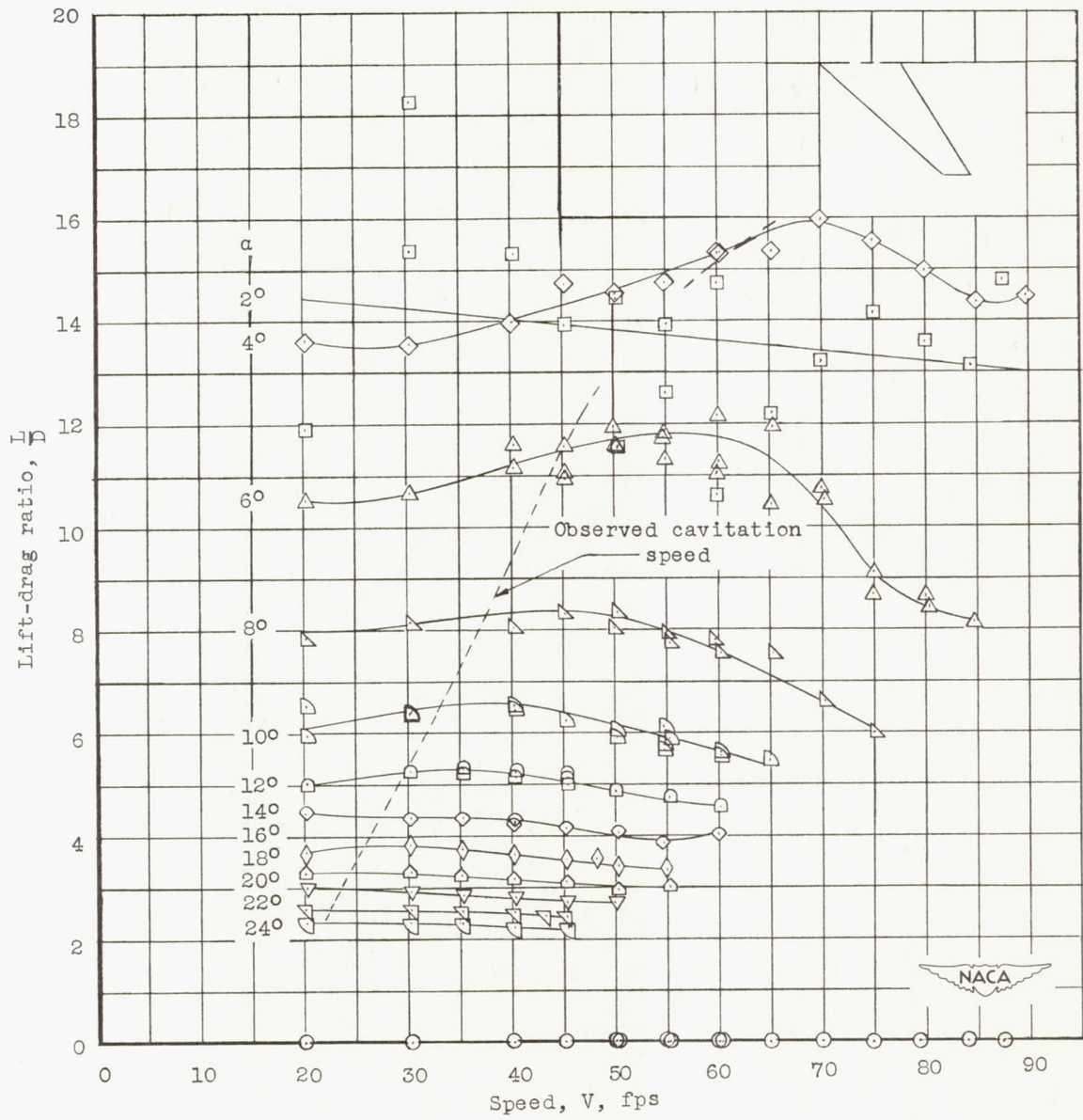
(c) Lift-drag ratio.

Figure 12.- Concluded.
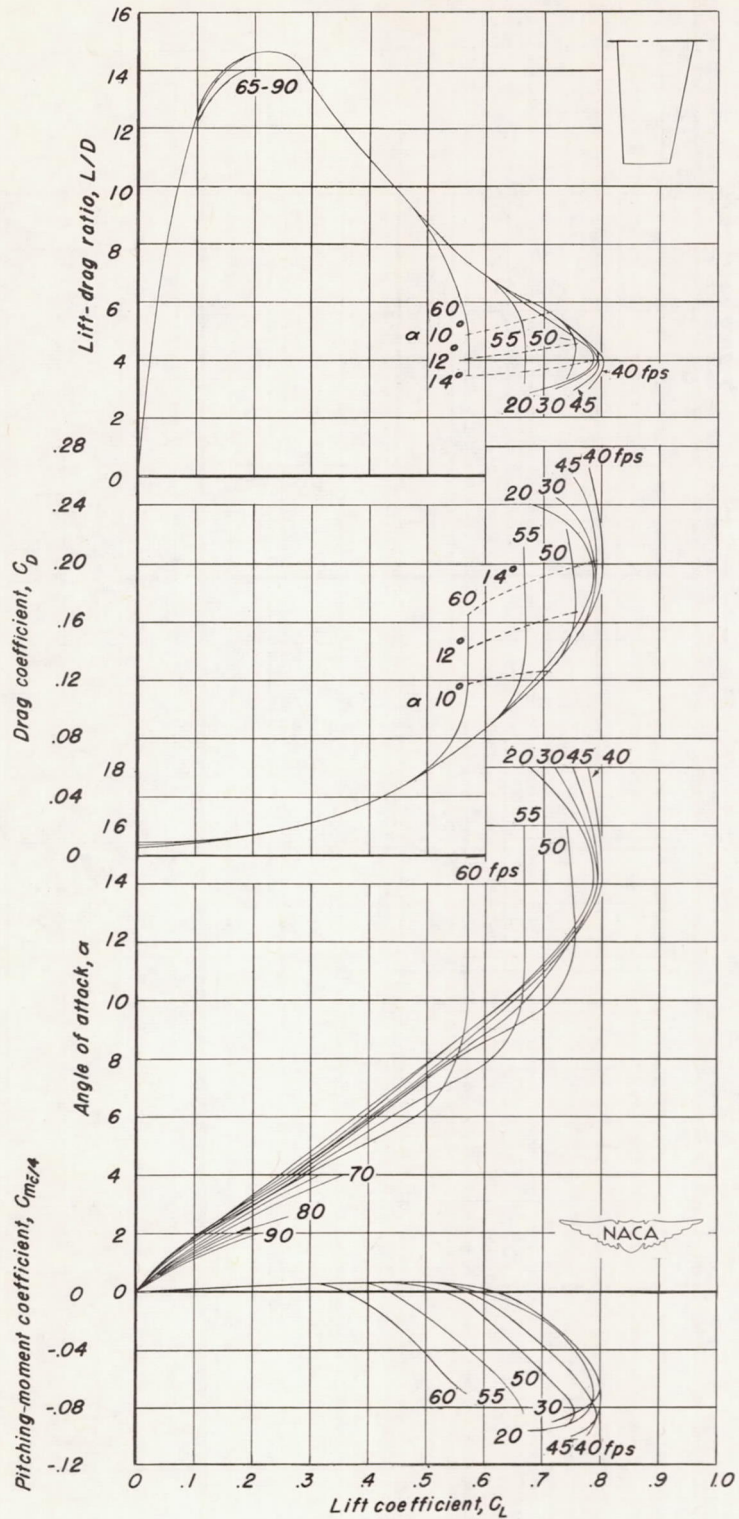
Figure 13.- Effect of speed on hydrodynamic characteristics
of 0-4-0.6 hydrofoil.
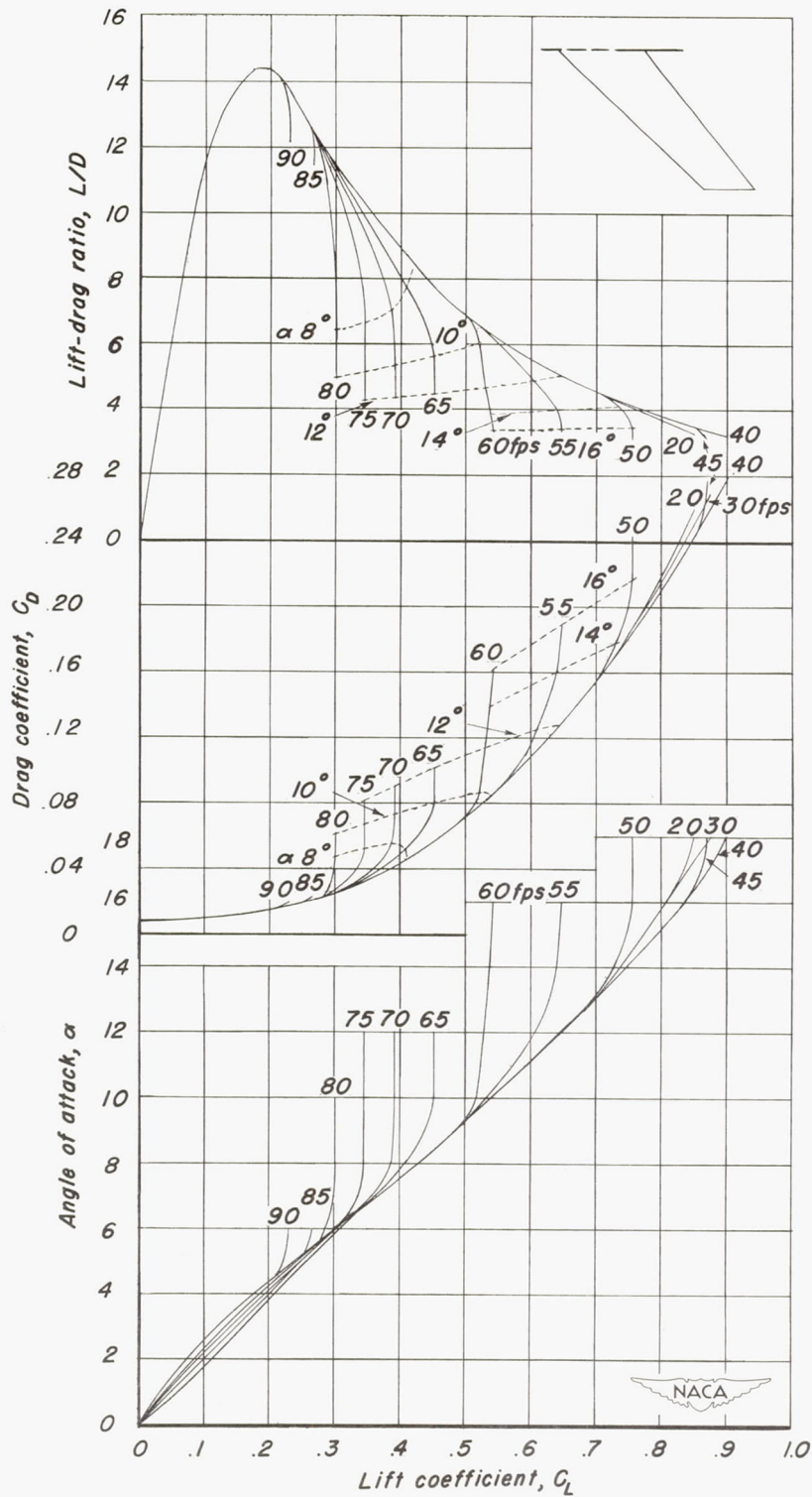
Figure 14.- Effect of speed on hydrodynamic characteristics
of 45-4-0.6 hydrofoil.
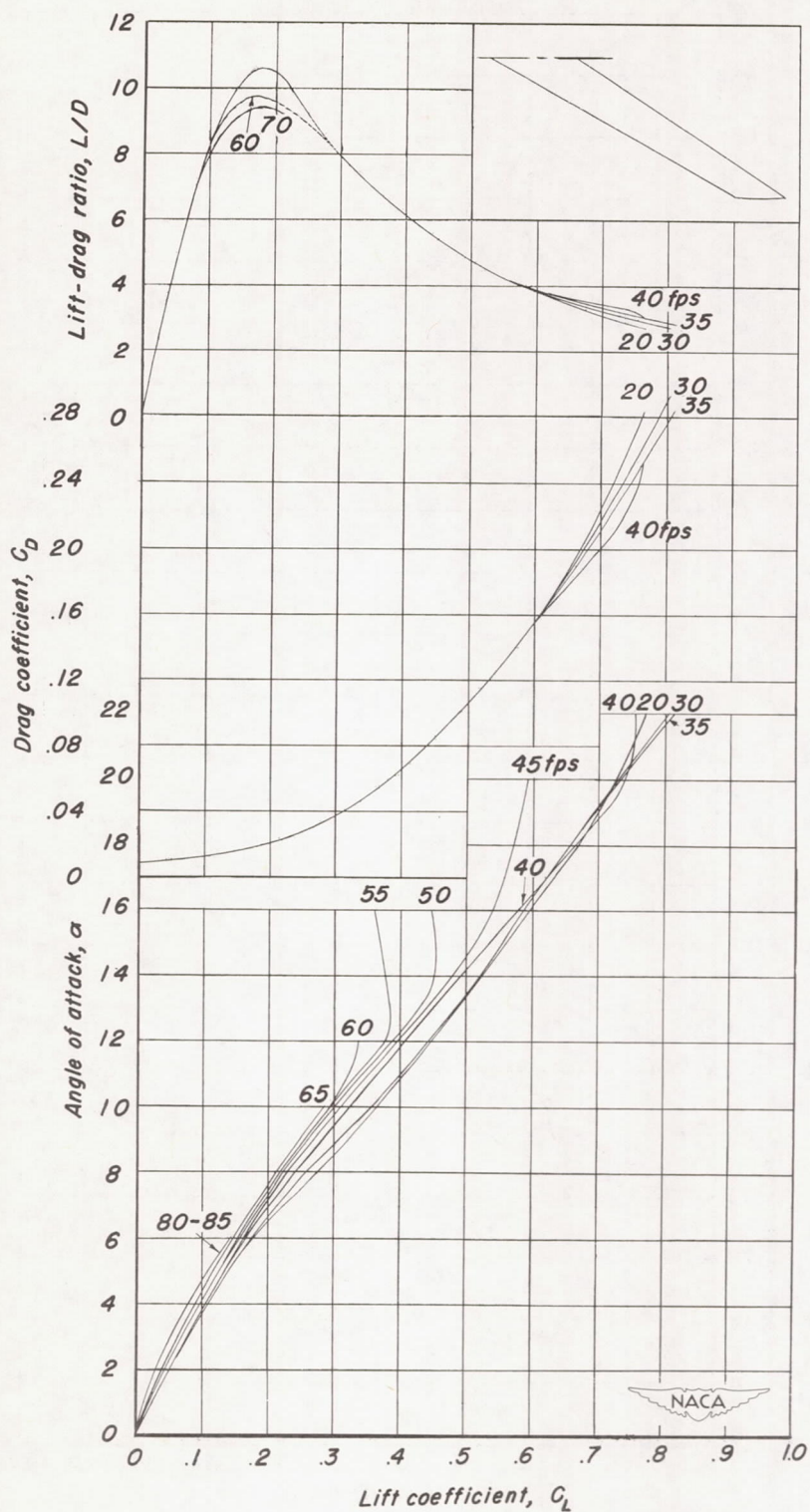
Figure 15.- Effect of speed on hydrodynamic characteristics
of 60-4-0.6 hydrofoil.
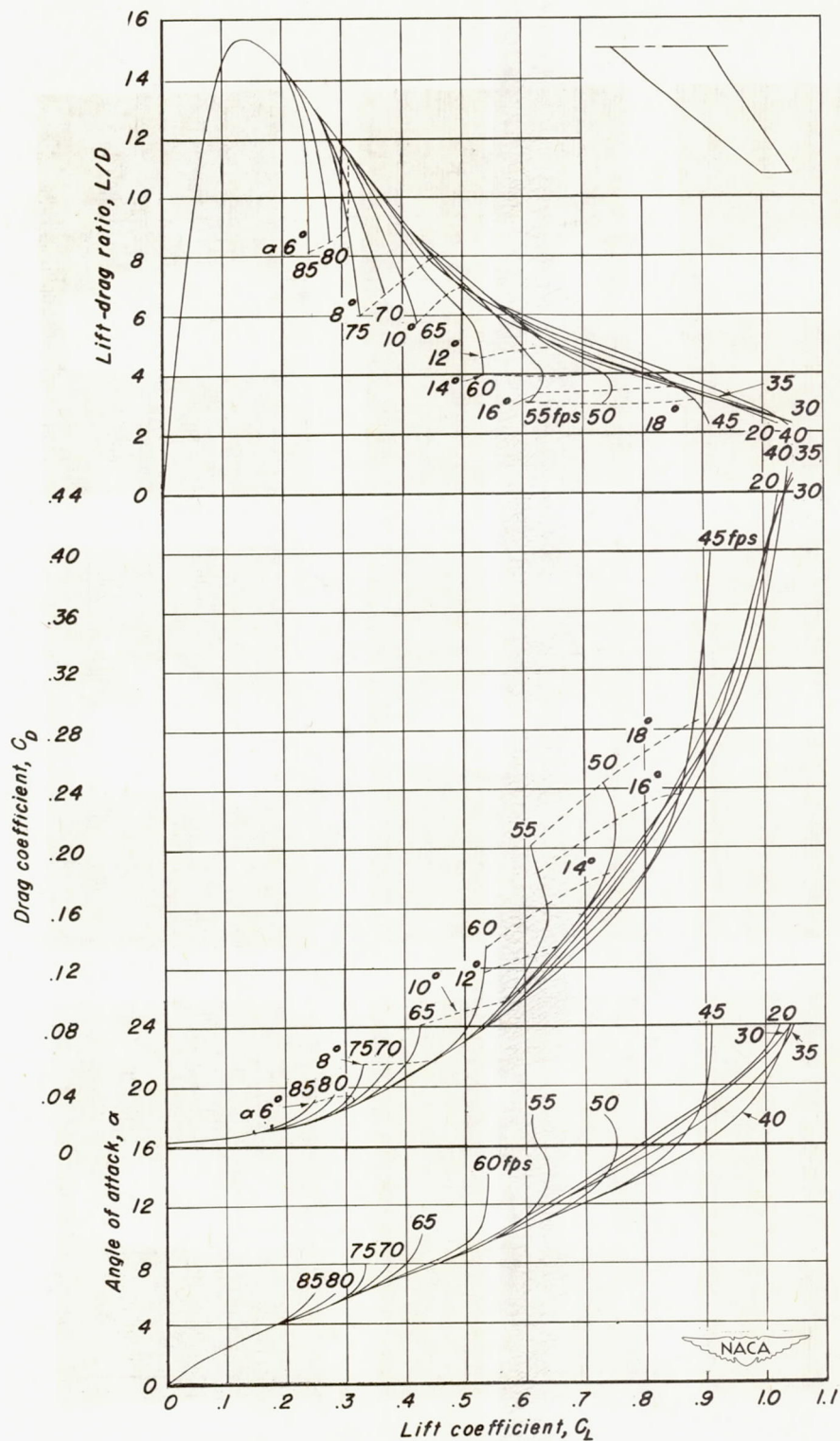
Figure 16.- Effect of speed on hydrodynamic characteristics of 45-4-0.3 hydrofoil.
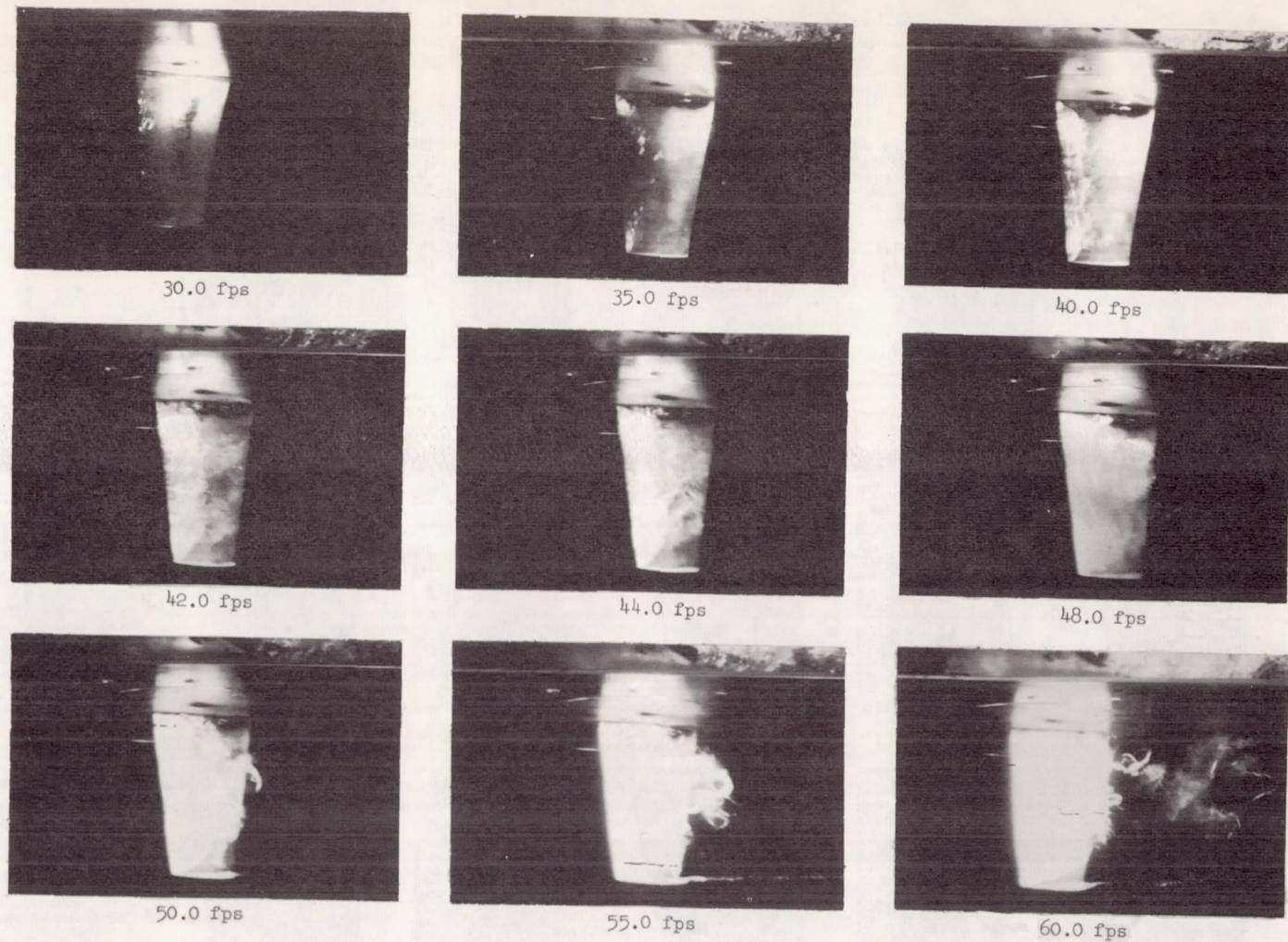
(a) 10° angle of attack.

Figure 17.- Appearance of cavitation on 0-4-0.6 hydrofoil.
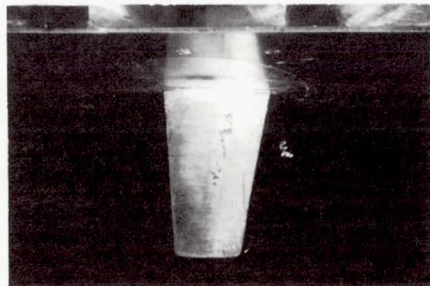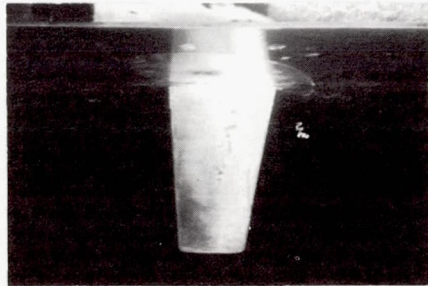
L-76958
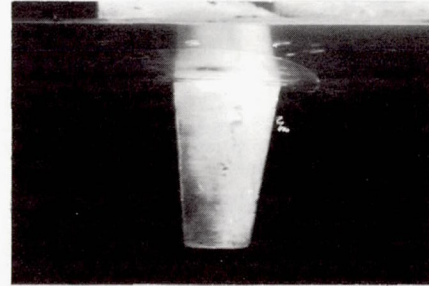
0 fps   30.4 fps   36.4 fps
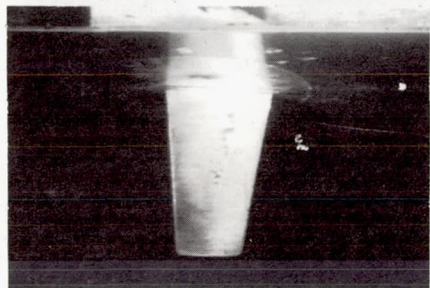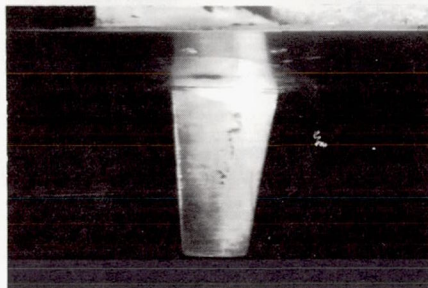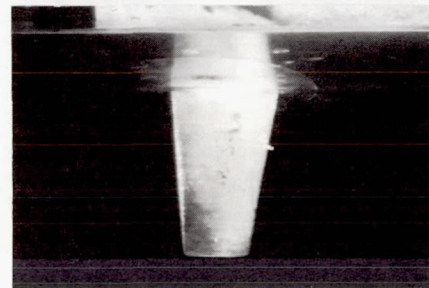
38.3 fps   40.5 fps   42.7 fps
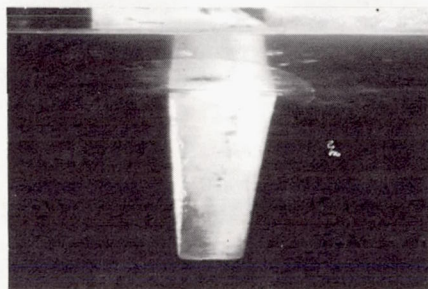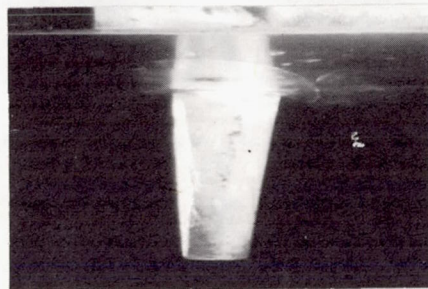
45.3 fps   50.0 fps

(b) 4° angle of attack.

Figure 17.- Concluded.

L-76959
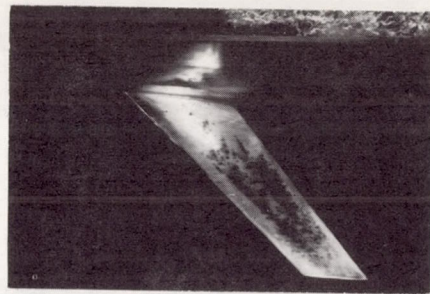
20.1 fps
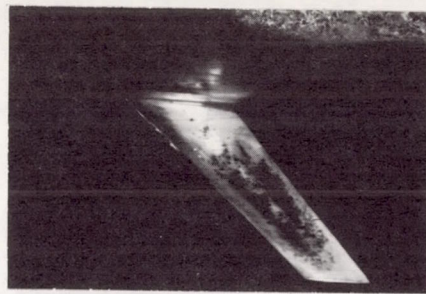
26.8 fps
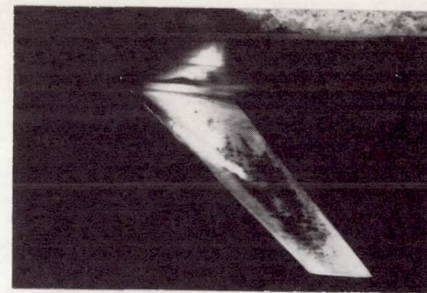
30.0 fps
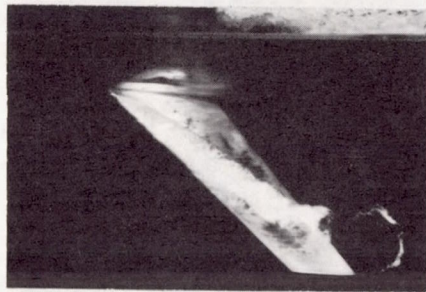
40.0 fps
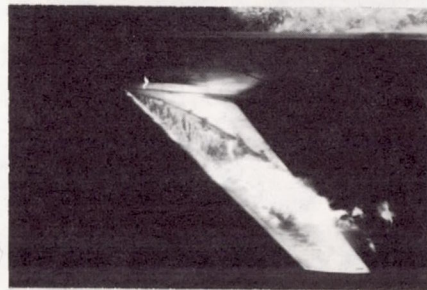
45.0 fps
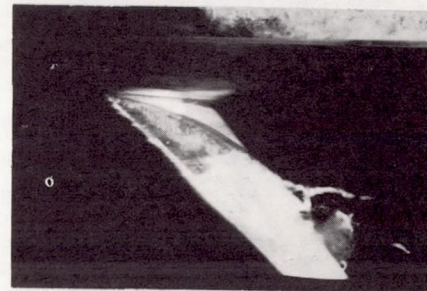
50.0 fps
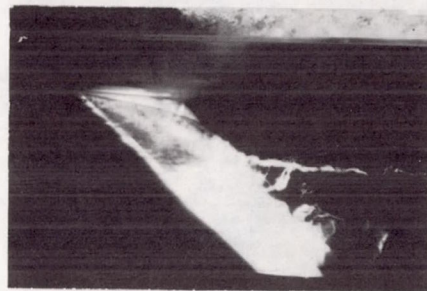
55.0 fps

(a) 14° angle of attack.

Figure 18.- Appearance of cavitation on 45-4-0.6 hydrofoil.

NACA
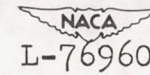
L-76960

36.2 fps   38.2 fps   39.3 fps
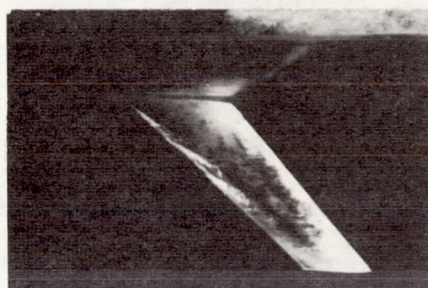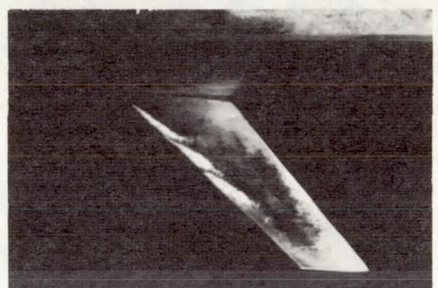
40.1 fps   42.1 fps   45.0 fps
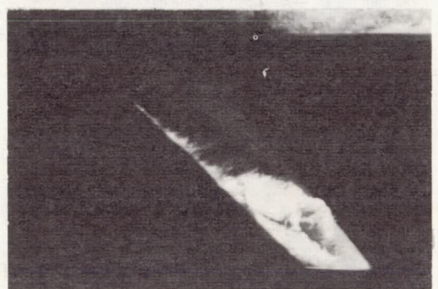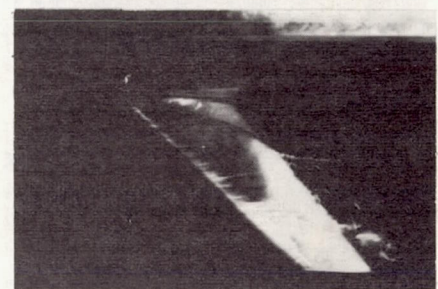
50.0 fps   60.0 fps   70.0 fps

(b) 8° angle of attack.

Figure 18.- Continued.
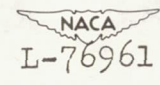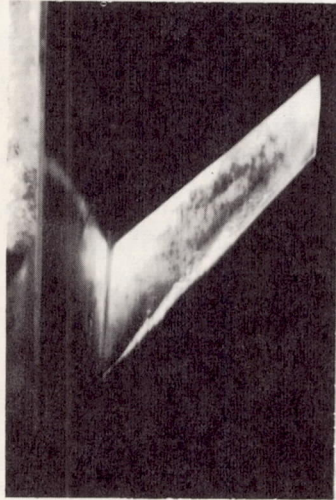
L-76961
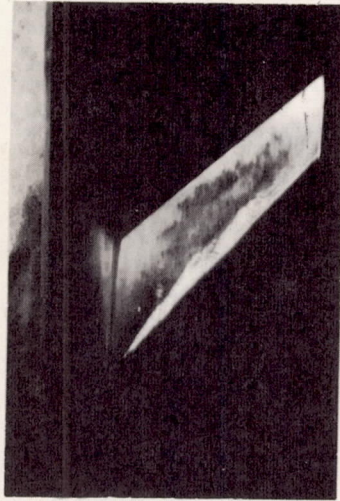
53.0 fps
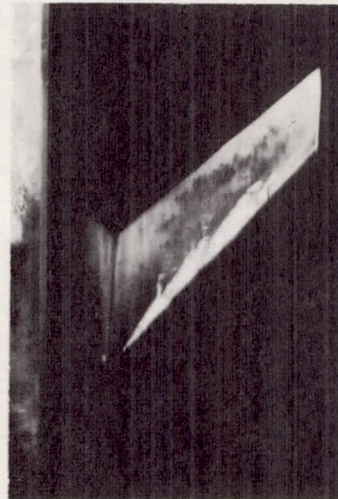
50.0 fps

40.0 fps

59.8 fps

54.8 fps
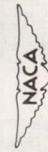
L-76962

(c) 6° angle of attack.

Figure 18.- Concluded.

31.1 fps	32.3 fps	33.3 fps
34.3 fps	40.3 fps	45.2 fps
50.0 fps	52.1 fps	55.0 fps
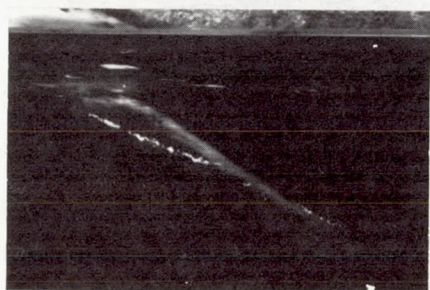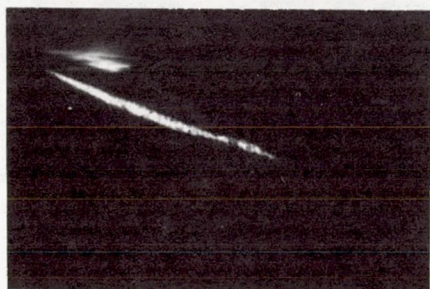
(a) 14° angle of attack.

Figure 19.- Appearance of cavitation on 60-4-0.6 hydrofoil.

L-76963

42.3 fps

44.3 fps

46.4 fps

48.3 fps

50.0 fps
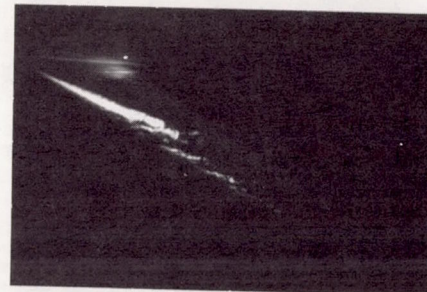
55.0 fps
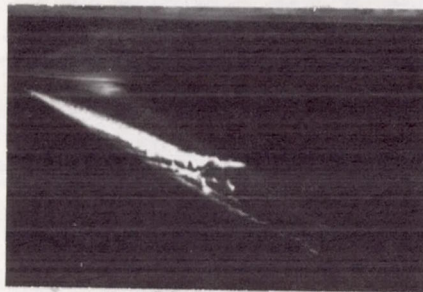
60.1 fps

(b) 10° angle of attack.

Figure 19.- Continued.
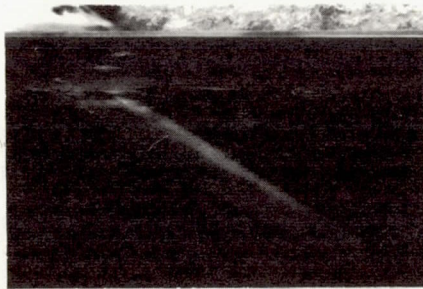
L-76964

40.3 fps   50.1 fps   60.2 fps
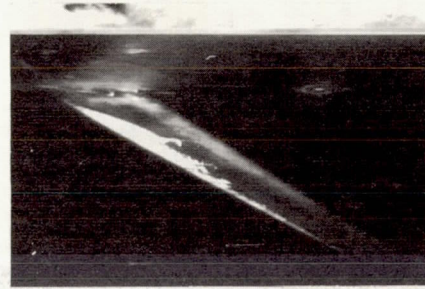
65.2 fps   70.1 fps   75.0 fps

80.0 fps

(c) 6° angle of attack.

Figure 19.- Concluded.

L-76965

20.3 fps

25.2 fps

30.3 fps

35.3 fps

40.4 fps

45.3 fps
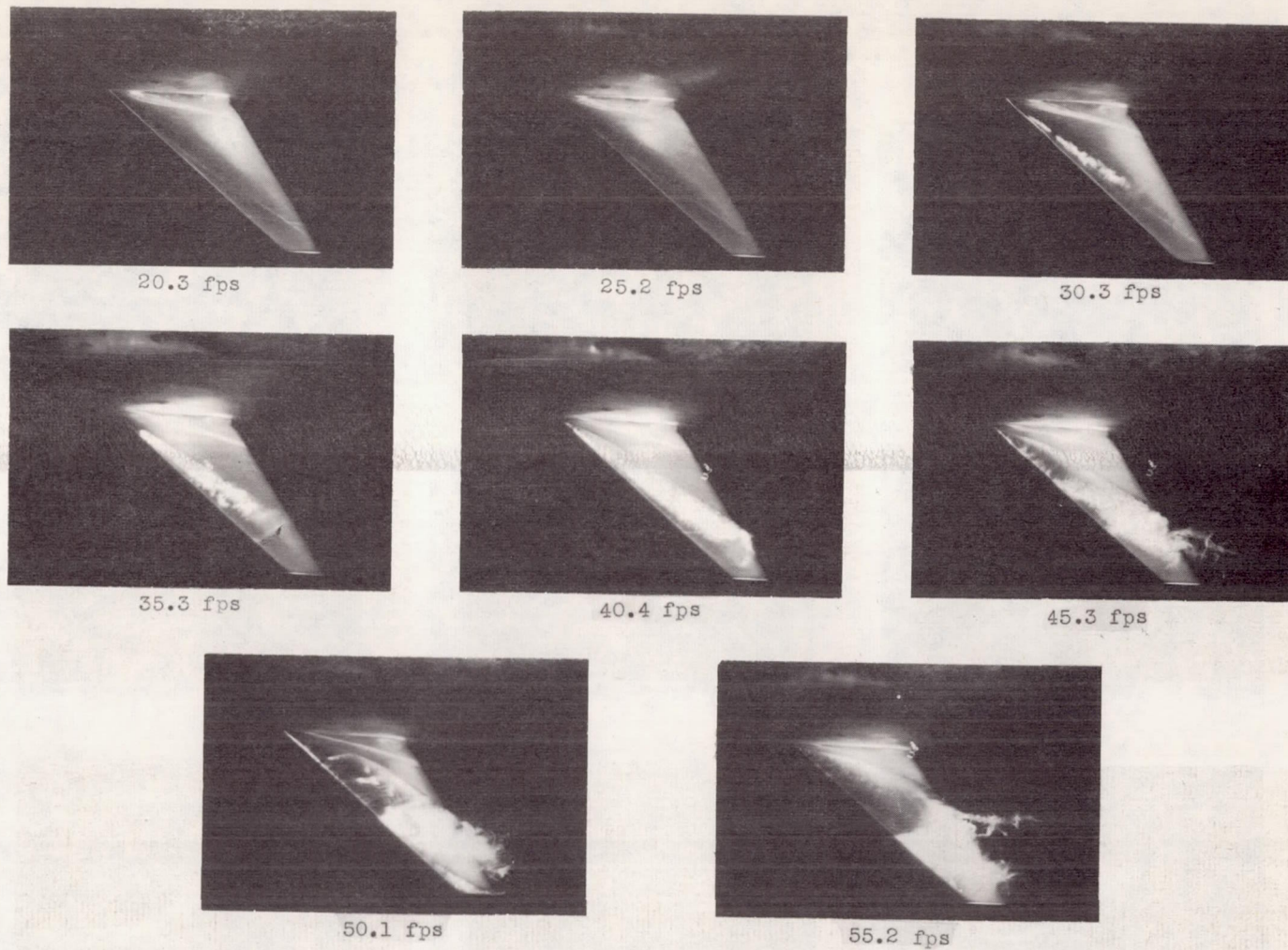
50.1 fps

55.2 fps

(a) 12° angle of attack.

Figure 20.- Appearance of cavitation on 45-4-0.3 hydrofoil.

NACA

L-76966

40.3 fps

45.2 fps

45.4 fps

50.1 fps

55.0 fps

60.1 fps

65.2 fps

70.2 fps

75.0 fps

(b) 6° angle of attack.

Figure 20.- Concluded.

L-76967
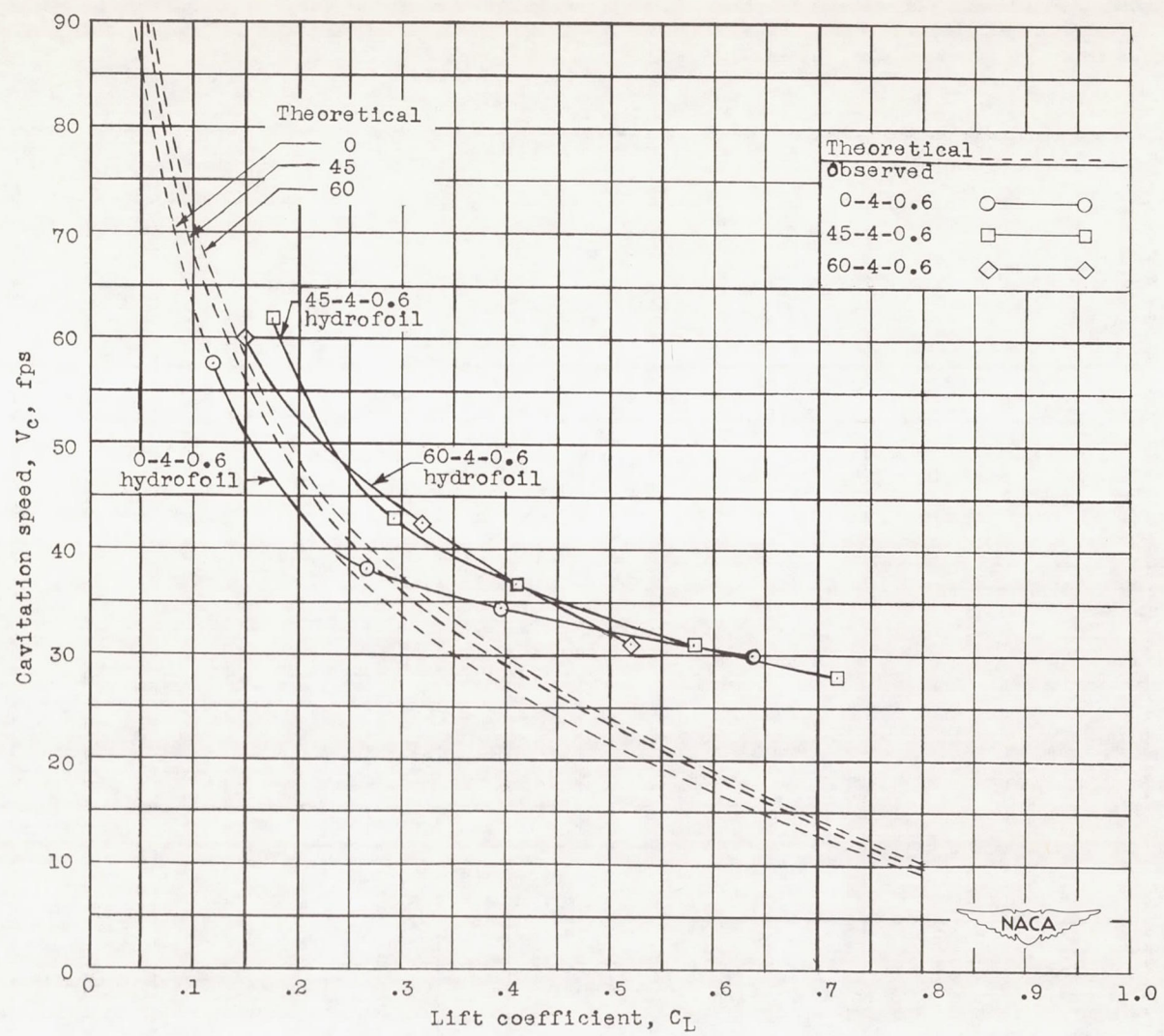
Figure 21.- Effect of sweep on cavitation speed.
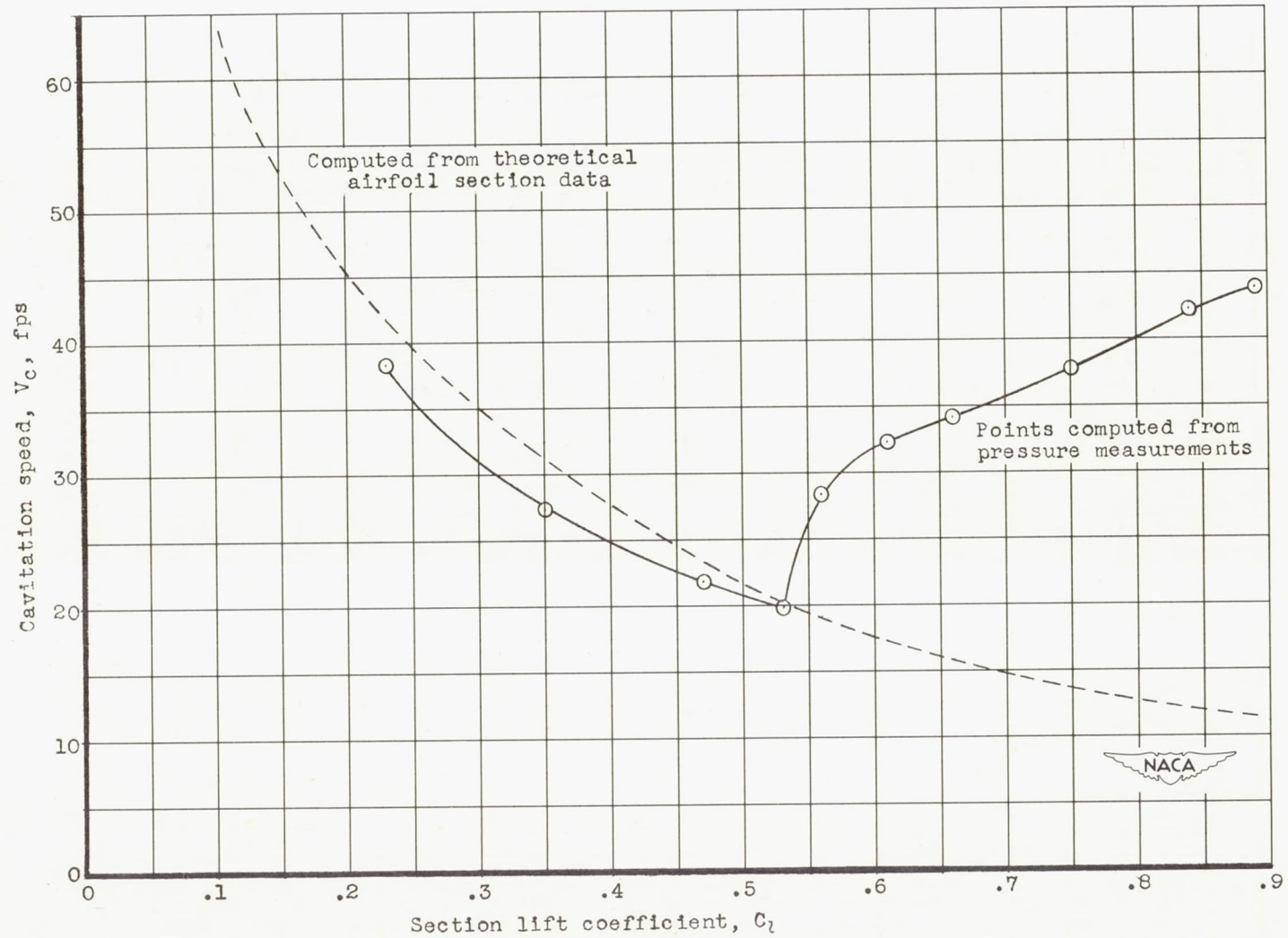
Figure 22.- Comparison of cavitation speeds computed from theoretical and experimental pressure distribution of NACA 64A006 airfoil section.
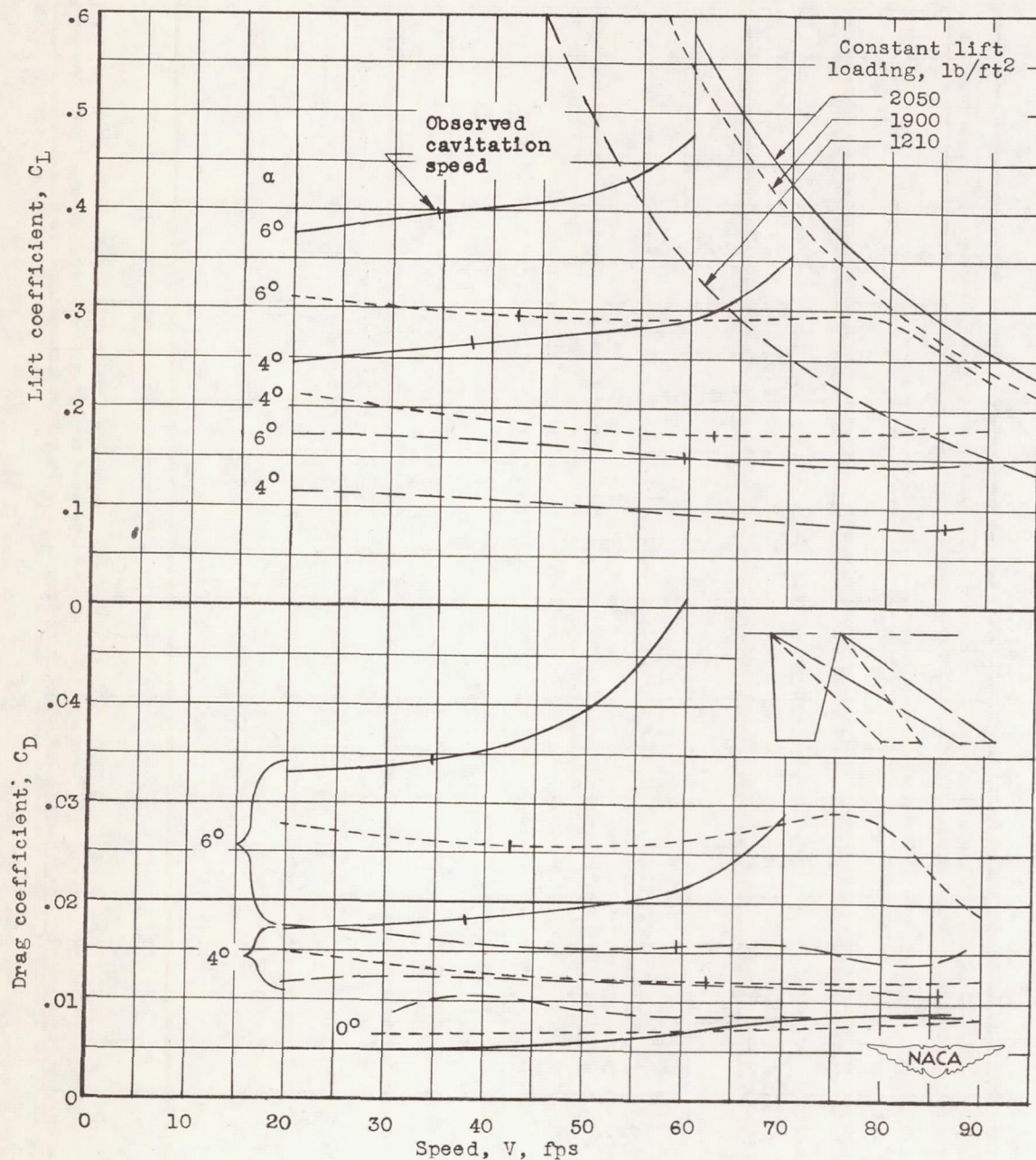
(a) At constant angle of attack.

Figure 23.- Effect of sweepback on hydrodynamic characteristics.
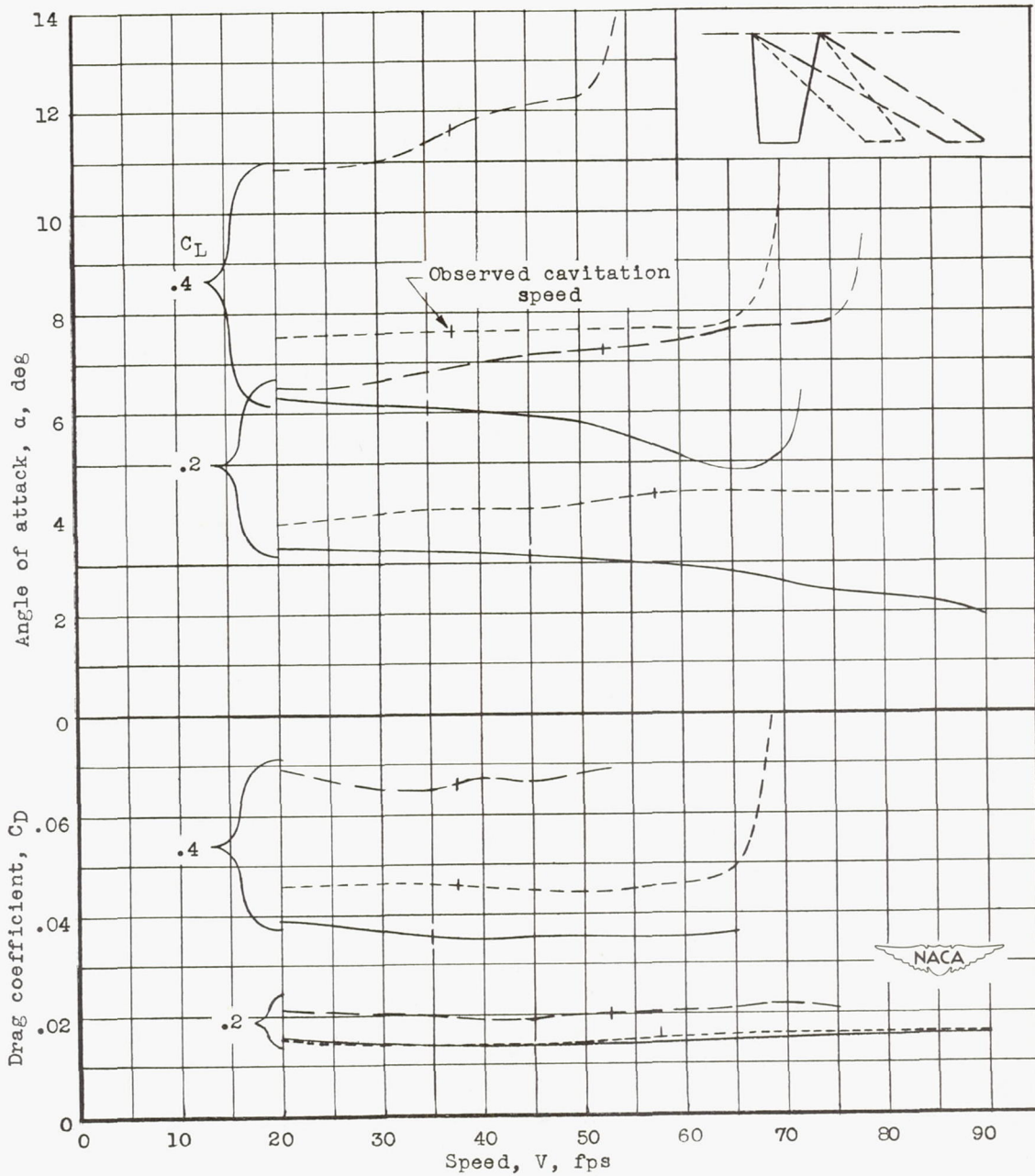
(b) At constant lift coefficient.

Figure 23.- Concluded.
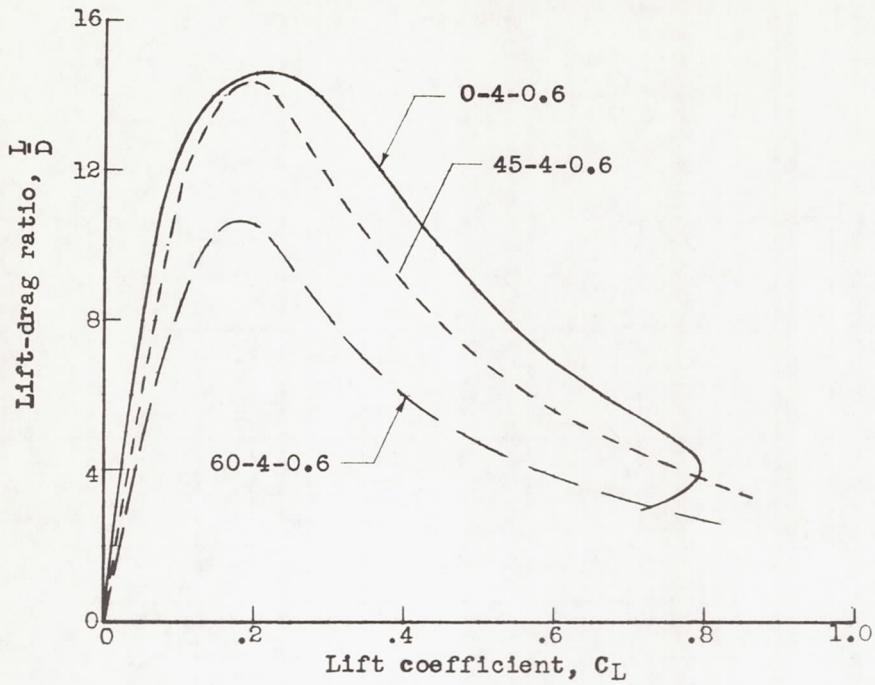
(a) Speed, 30 feet per second.
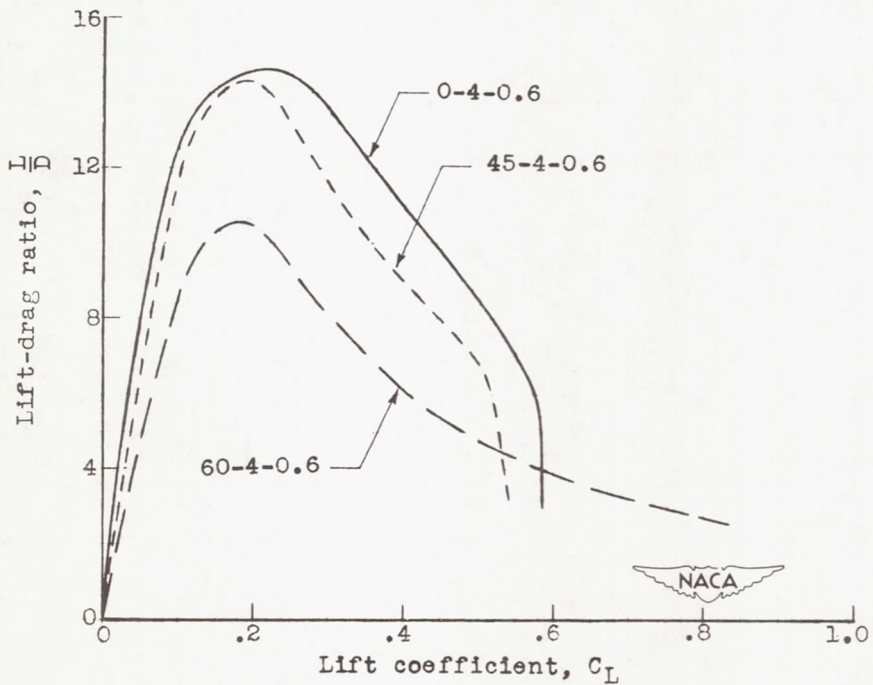
(b) Speed, 60 feet per second.
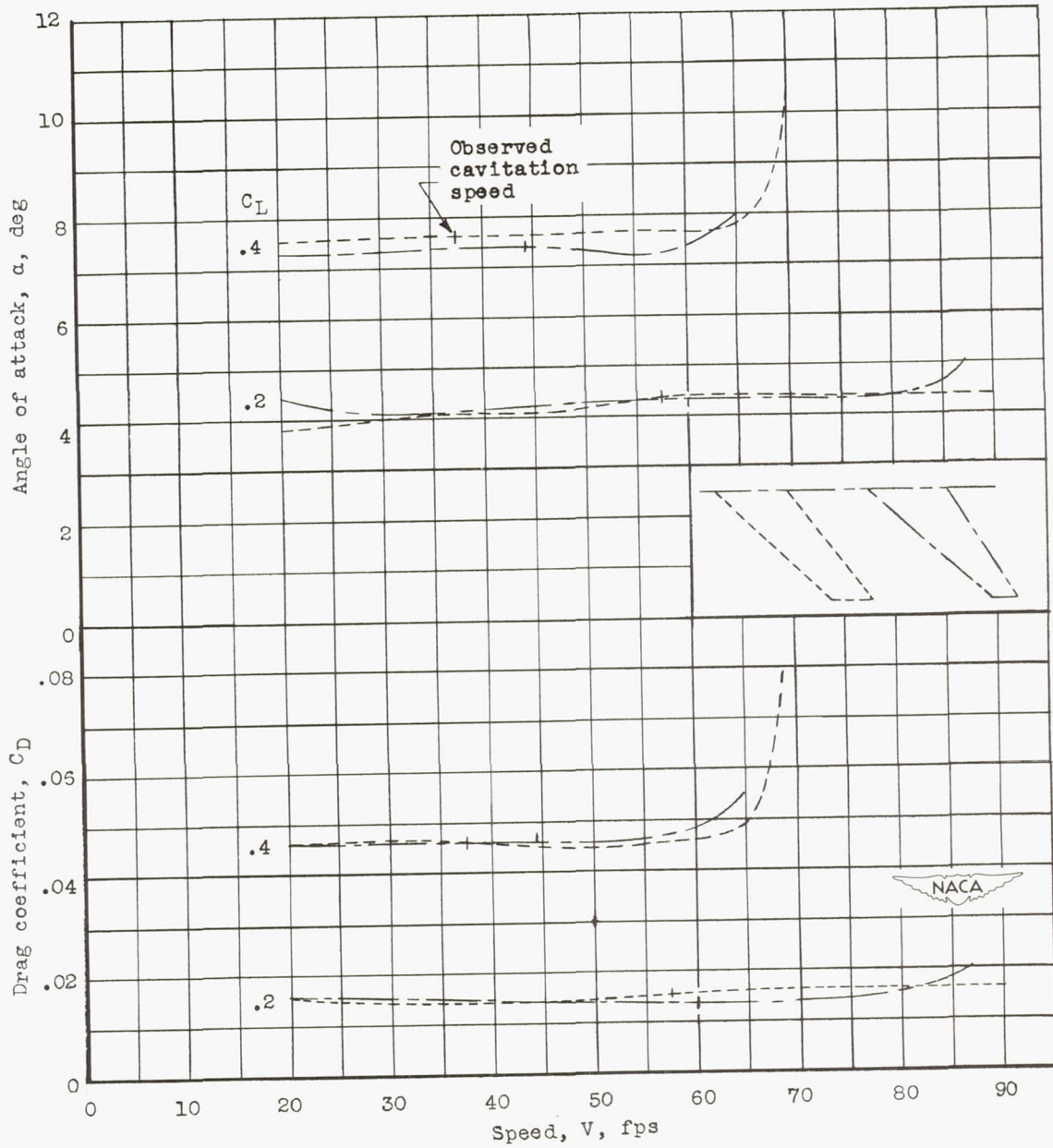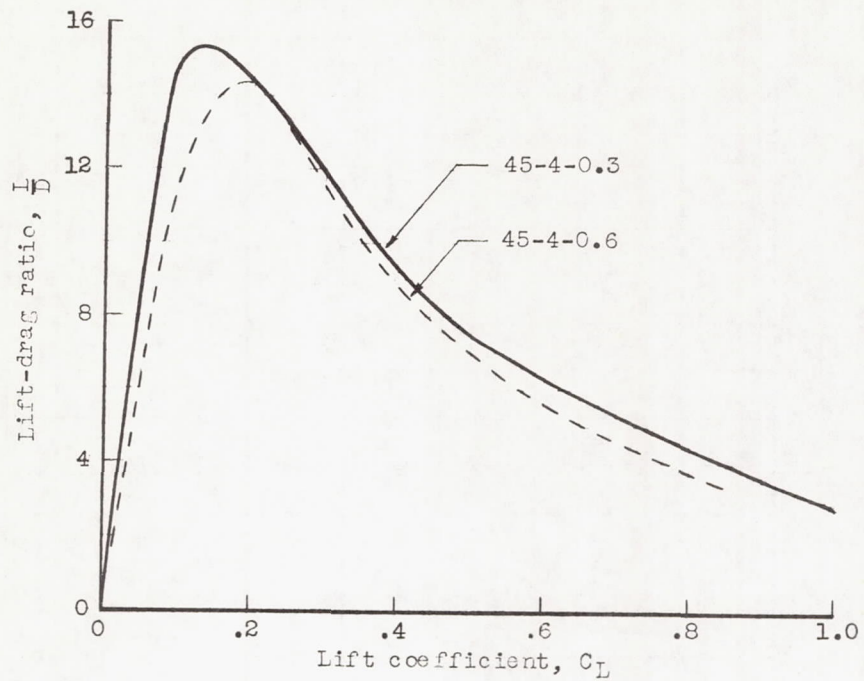
Figure 24.- Effect of sweep on lift-drag ratio.
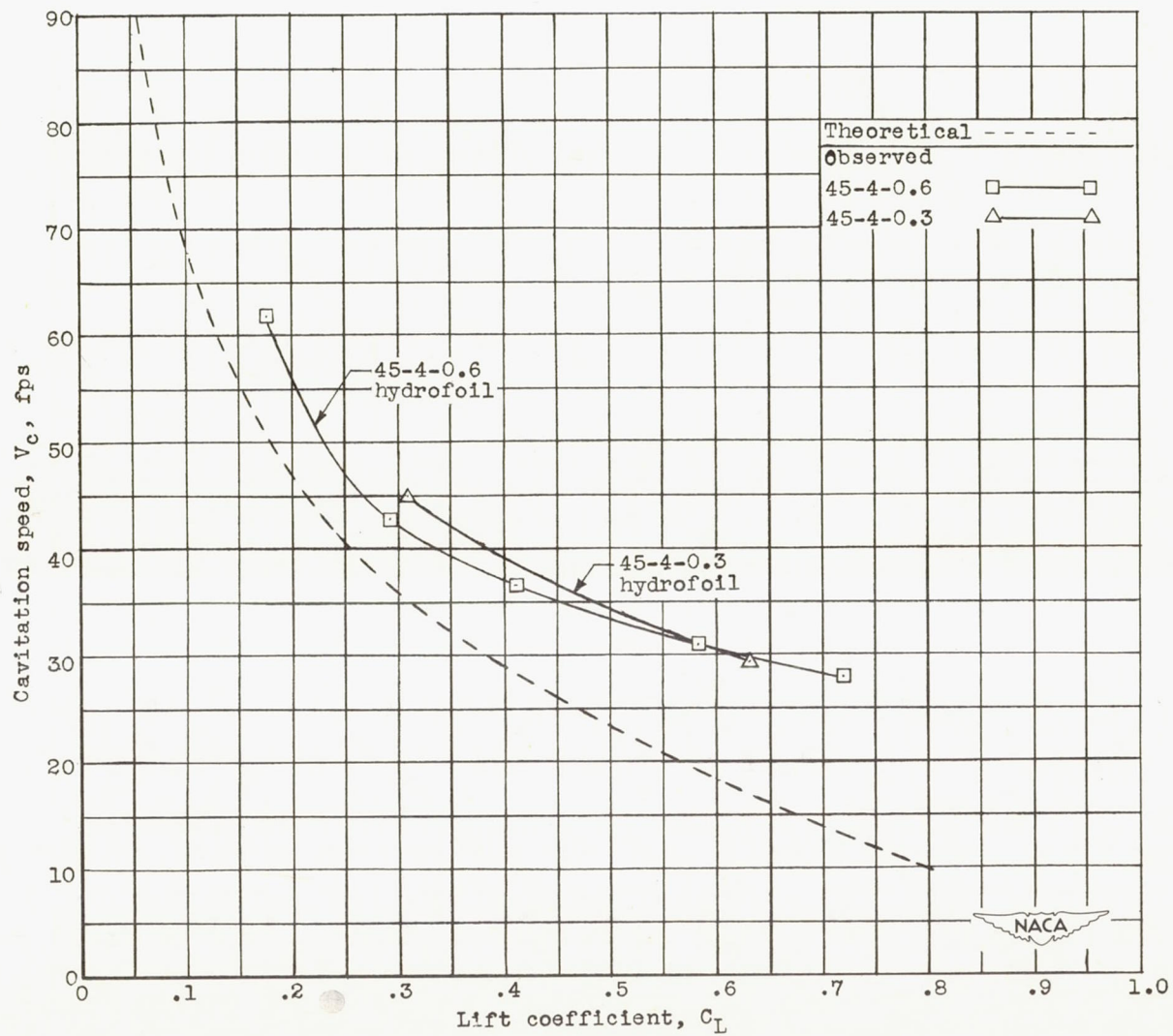
Figure 25.- Effect of taper ratio on cavitation speed.
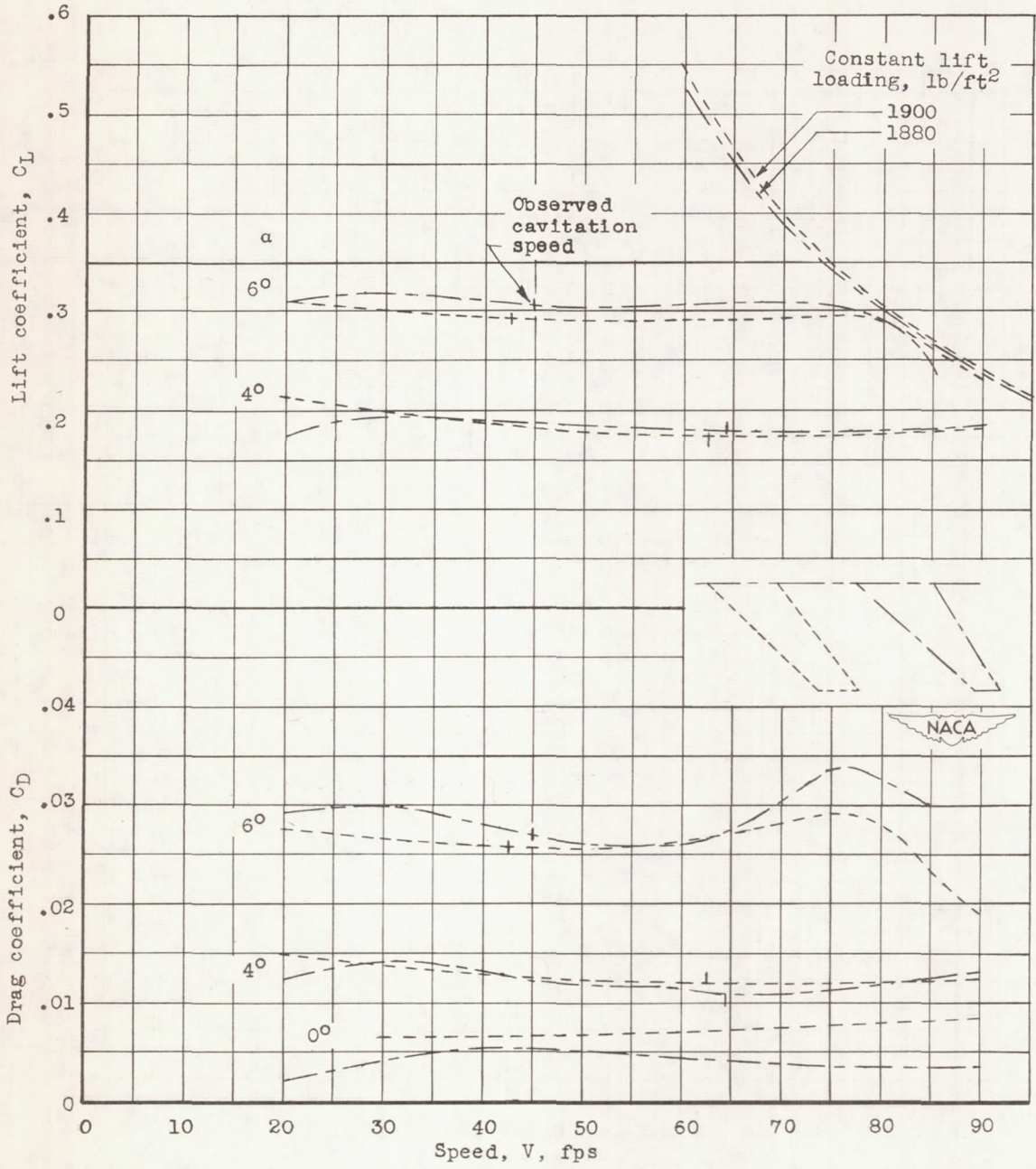
(a) At constant angle of attack.

Figure 26.- Effect of taper ratio on hydrodynamic characteristics.

(b) At constant lift coefficient.
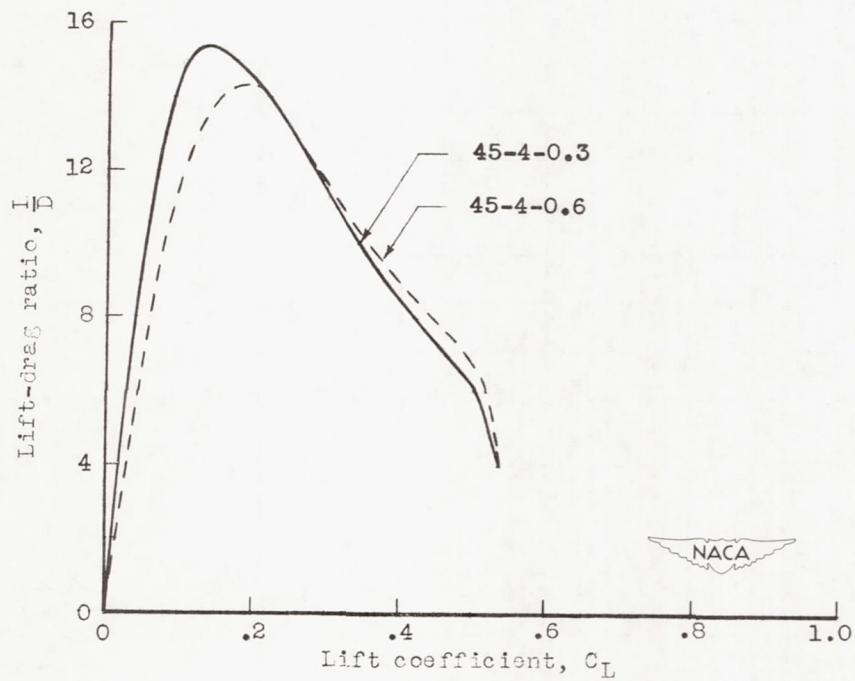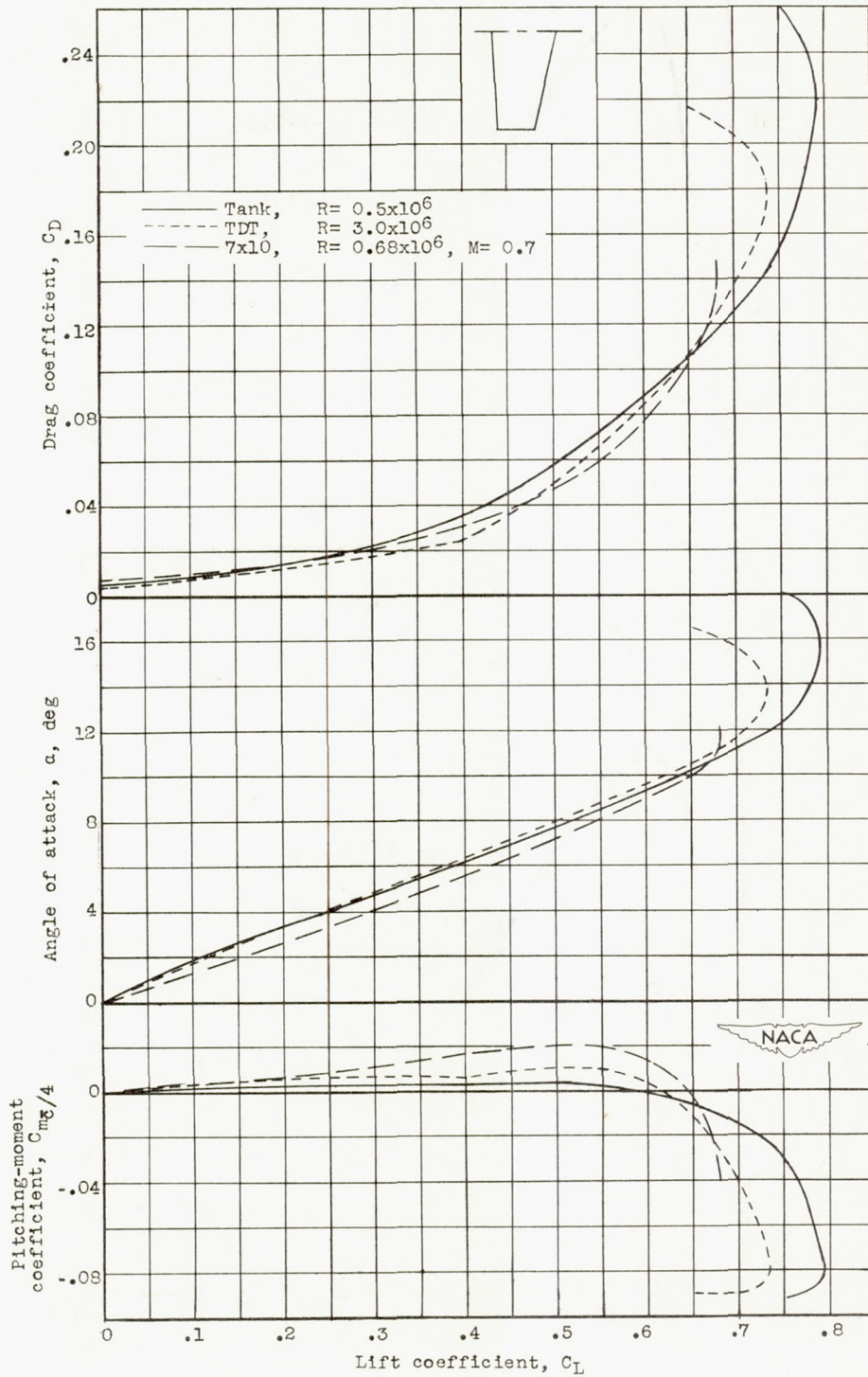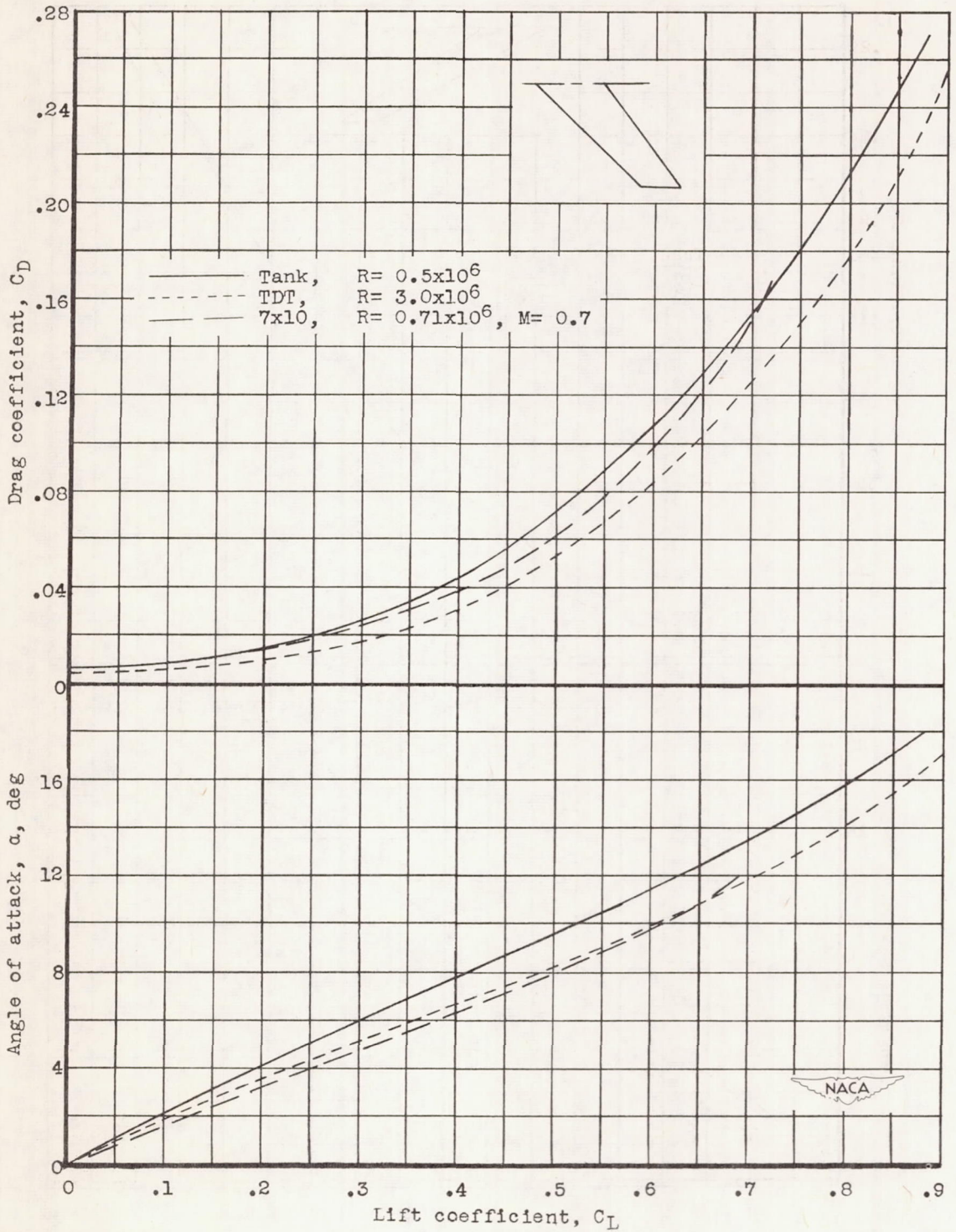
Figure 26.- Concluded.

(a) Speed, V, 30 feet per second.

(b) Speed, V, 60 feet per second.

Figure 27.- Effect of taper on lift-drag ratio.

(a) 0-4-0.6 hydrofoil and wing.

Figure 28.- Comparison of hydrodynamic characteristics of hydrofoils at
subcavitation speeds and aerodynamic characteristics of similar wings.
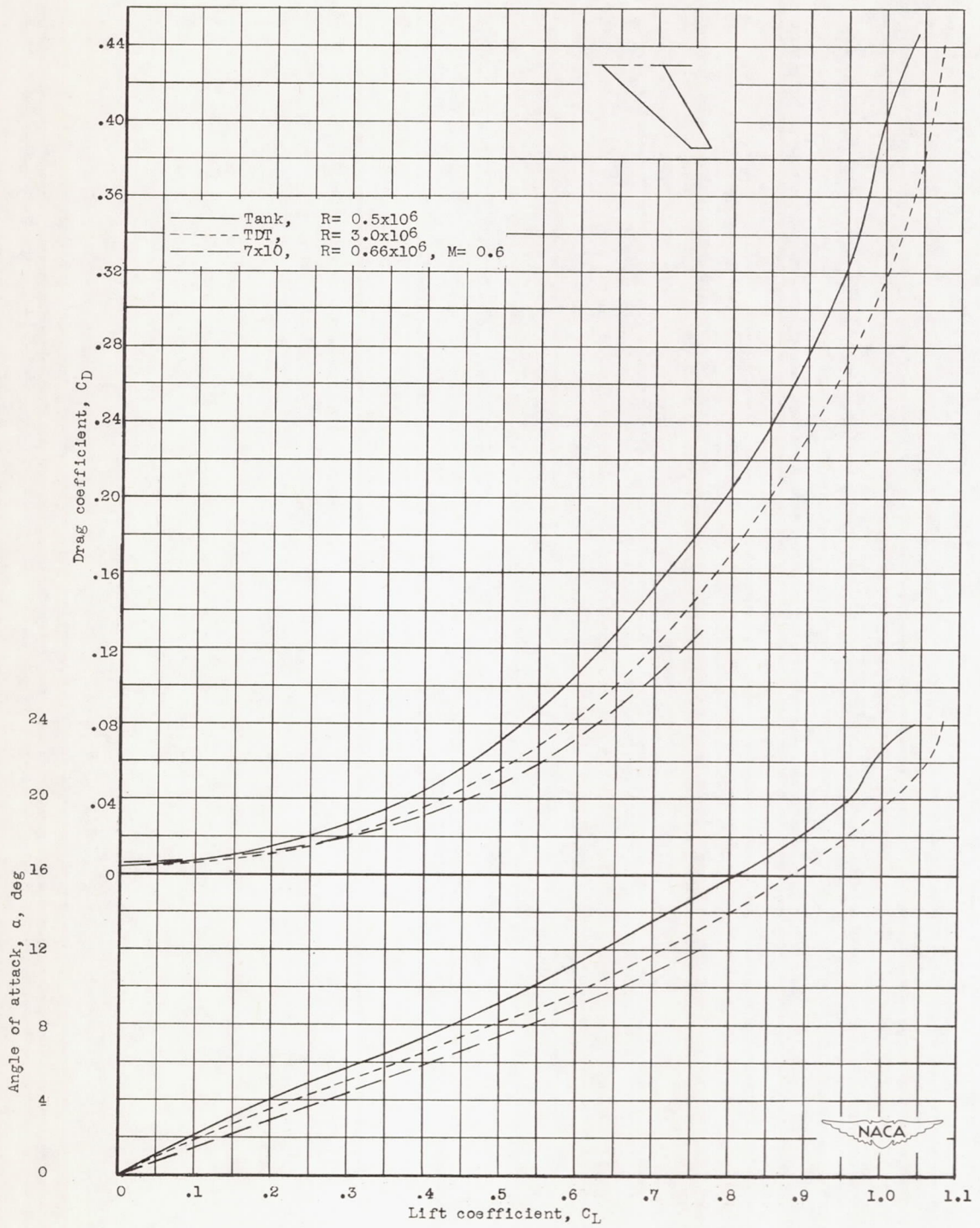
(b) 45-4-0.6 hydrofoil and wing.

Figure 28.- Continued.

(c) 60-4-0.6 hydrofoil and wing.

Figure 28.- Continued.

(d) 45-4-0.3 hydrofoil and wing.

Figure 28.- Concluded.